J. Fluid Mech. (1976), *vol.* 78, *part* 4, *pp.* 641–676
Printed in Great Britain

Measurements of interacting turbulent shear layers in a duct

By R. B. DEAN
Atkins Research and Development, Epsom, Surrey
AND P. BRADSHAW
Department of Aeronautics, Imperial College, London

(Received 23 April 1976)

Measurements have been made of the turbulent flow in a rectangular duct of aspect ratio 12:1 at a Reynolds number $\bar{U}h/\nu = 10^5$ (based on duct height h) using conditional-sampling techniques. The lower boundary layer was heated in the entry region, and the fluctuating output of a resistance thermometer was used to distinguish 'hot' and 'cold' fluid. Thus separate velocity-fluctuation statistics could be obtained for fluid from the upper and lower boundary layers, even after the two layers had merged. The measurements suggest that the interaction region near the centre-line consists of a continuously contorting interface between the 'hot' and 'cold' layers, shaped by the eruption of large eddies across the centre-line from either side of the duct and surprisingly little affected by the inevitable fine-scale mixing.

In the mean, this time-sharing between 'hot' and 'cold' fluid gives the impression of two superposed turbulence fields whose mean-square intensities add to give the total intensity. Exact superposition (which cannot take place in a nonlinear system) would imply that one layer had the same turbulent intensity profiles as an isolated boundary layer spreading into a non-turbulent free stream with the same mean velocity profile as the duct flow. The centre-line interaction grows in strength with increasing distance downstream until a steady rate of mutual eddy intrusion and fine-scale mixing is achieved, when the flow is commonly called 'fully developed'. It is concluded that superposition (time-sharing) is a physically reasonable first approximation for use in turbulence models for interacting shear layers: it is argued that better approximations could be obtained if necessary by correlating departures from superposition (i.e. changes in turbulence structure) by means of one or more interaction parameters.

1. Introduction

Nearly all complex turbulent flows can be described as perturbations of simple shear layers, either by interaction with other shear layers or by the imposition of body forces or extra rates of strain (additional to the simple shear $\partial U/\partial y$). The simplest kind of shear-layer interaction occurs between two layers with shear stress of opposite sign, separated by a plane of zero mean shear, such as the two halves of a wake or jet or the inlet region of the flow in a duct. Bradshaw, Dean &

McEligot (1973) have successfully extended the boundary-layer calculation method of Bradshaw, Ferriss & Atwell (1967) to rectangular duct flow by assuming that the turbulence fields of the two shear layers may be directly superposed, interaction taking place via the mean velocity profile only. The shear-stress gradient in the overlap region is determined by simply adding the shear-stress gradients of the two layers as if each existed in the absence of the other. The work of Bradshaw, Dean & McEligot was carried out during the course of the present investigation and the early experimental results were used to support their theoretical assumptions. The Navier–Stokes equations, being nonlinear, do not allow exact superposition but it is argued that superposition should be a reasonable first approximation if the effects of the interaction on the turbulence structure are weak. This approach is possible only with calculation methods that do not relate the shear stress directly to the mean velocity profile but allow for turbulent transport of stress from elsewhere. That is, it is usable only with transport-equation methods and not with eddy-viscosity methods.

This paper describes some† of the results of an investigation to explore the superposition hypothesis and to determine the strength and extent of the interaction near the centre-line of a symmetrical rectangular duct of high aspect ratio. The interaction mechanism is likely to be virtually the same in a symmetrical flow as an asymmetrical one; symmetry just disguises the more striking results of the interaction. Examples of asymmetrical quasi-plane interactions include the wake of a lifting aerofoil, the flow in an annular duct and the wall jet. More complicated, multiple interactions occur on aerofoils with slotted flaps and in the rolling up of spanwise or longitudinal vortices. However the 'two-dimensional' symmetrical rectangular duct flow avoids the introduction of arbitrary complications and allows attention to be concentrated on the interaction itself. It is not suggested that the results are necessarily relevant to the problems of non-coplanar interactions such as occur in the streamwise corners of ducts, or to axisymmetric flows like the circular pipe investigated by Sabot & Comte-Bellot (1976).

Primarily, the object of the present work is to follow the intrusion, across the centre-line, of eddies originating from either shear layer and to distinguish from which layer each has come. This permits an assessment of the extent to which the two layers are interacting with each other, particularly the distance from the centre-line to which the interaction penetrates, and also permits the turbulence structure (dimensionless parameters) to be compared with measurements in an isolated boundary layer. The experimental technique developed to perform this task involves the application of sufficient heat to the lower boundary layer to permit discrimination from the top, unheated layer by a fast-response wire resistance thermometer. The intermittent temperature signal obtained near the duct centre-line is recorded on analog magnetic tape, together with simultaneous velocity signals from a cross-wire hot-wire probe close to the resistance-thermometer wire. The signals are later replayed from analog tape into an analog-to-digital conversion system and transferred in digital form to a second magnetic

† The complete set of results, a full description of experimental techniques, and details of the modifications to the calculation method are given by Dean (1974*a*).

tape. The digital tape is then input to a large computer so that statistical properties of the signals can be obtained.

Section 2 describes the test rig in which the investigation was carried out and §3 explains the special experimental techniques required for conditional sampling based on temperature intermittency. The criteria used to distinguish bursts of heated fluid from unheated ('cold') fluid are introduced in §4 and the details of the measurements taken near the duct centre-line are fully described. The results obtained by application of these techniques are discussed in §§5–7. The main emphasis in the analysis is on the extent of overlap between the two shear layers (§5), which provides information about the interaction mechanism. By comparing the present data with conditionally sampled measurements in a constant-pressure boundary layer, it is shown in §6 that the effect of the favourable pressure gradient, as such, on the turbulence structure is negligible. In §7, comparisons of the main structural parameters with boundary-layer measurements show that superposition of the turbulence fields of each shear layer gives an adequate description of the interaction processes near the centre-line of the duct. The reason for this surprising conclusion is quite simple: the interaction takes place in what would be the intermittent region of an isolated boundary layer, and the large-eddy eruptions from one layer 'time-share' with those from the other layer as sketched in figure 6 below. Evidently, the continual exchange of fluid from one side of the duct to the other takes place via fine-grained mixing of low-intensity fluid near the edges of the eruptions, rather than by violent interactions involving the whole large-eddy structure. In the mean, 'time-sharing' is indistinguishable from superposition. The implications for calculation methods are discussed in §8.

2. Experimental arrangement

The duct, 60×5 cm in cross-section, is supplied by air by a 3 kW blower via a settling chamber and a 9:1 two-dimensional contraction (figure 1) with a trip wire at the downstream end. The measurements were made at an area-mean flow speed $\overline{U}$ of $30\,\mathrm{m\,s^{-1}}$ (Reynolds number $\overline{U}h/\nu = 10^5$) with a turbulence intensity $(\overline{u^2})^{\frac{1}{2}}/\overline{U}$ of about 0·001 at the entry to the duct. Pitot tubes and hot-wire probes, mounted on electrically driven traverse gear, were introduced through ports in the floor of the duct at stations A–P (figure 1). The reference speed U_{ref} is that at $x = 0$, $y = \frac{1}{2}h$ and is close to $\overline{U}$.

Longitudinal turbulence intensity was determined using a DISA U-probe, with a 5 μm platinum wire, whilst all measurements of the normal and spanwise turbulence components were performed by a DISA miniature cross-wire probe (55A38) with the gap between the two wires increased to 1 mm so as to avoid any possible effects of thermal wake interference (Guitton & Patel 1969). The yaw response of the cross-wire probe was obtained by determining the 'effective' angles between the flow direction and the planes normal to the wire axes [the method recommended by Bradshaw (1971) and described by Dean (1974*a*)]. Each wire was calibrated by the conventional (static) procedure. Comparisons of static and dynamic calibrations have been made by Chandrsuda (1976) using

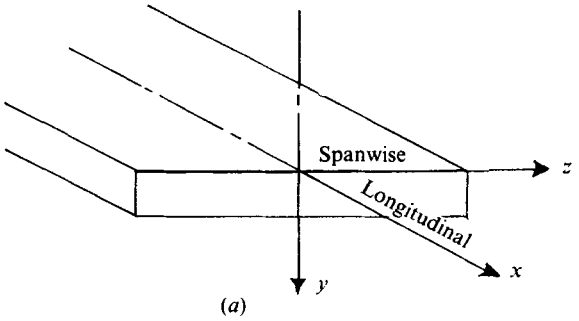

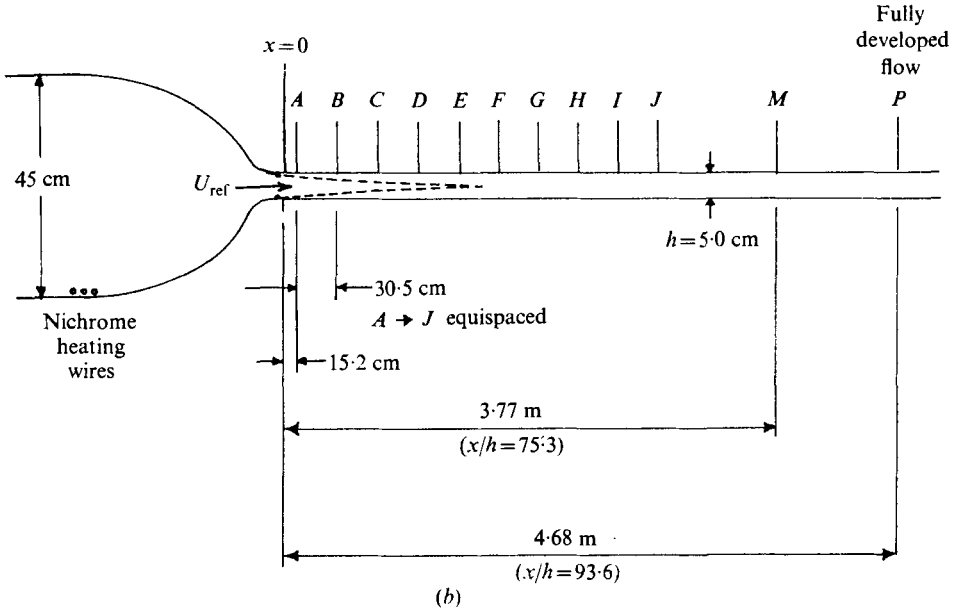

FIGURE 1. The 'two-dimensional' duct. (*a*) Co-ordinate axes. (*b*) Nominal dimensions.

the same types of probe: similar deviations from the 0·45 power version of King's law are found in both static and dynamic calibrations but the implied errors in the present experimental results are not more than 5% of mean-square intensity because the mean velocity range (and therefore the range of values of $\partial E/\partial U$) is rather small. The DISA anemometer 55D01, r.m.s. voltmeter 55D35 and auxiliary unit were used for signal processing with all hot wires in conjunction with operational amplifiers, which provided the sums and differences of signals as well as conventional amplification where required. The signals were linearized after digitization by the data reduction program CS4-A, which is discussed in §3. Measurements of the mean flow and basic turbulence quantities agreed well with the results of previous workers (for a review, see Dean 1974*b*).

3. A conditional-sampling technique

Many investigations of the intermittent regions of turbulent shear flows have been published in recent years. Thomas (1973) provides a nearly comprehensive list of authors and some details of more recent work are given below. The purpose of most of these studies has been to attempt an explanation of the mechanism of entrainment of non-turbulent fluid by the turbulent flow field, and to provide separate statistical information on each zone. The feature common to all such investigations involving the discrimination of a turbulent/non-turbulent interface is the need to determine a time-resolved function which has markedly different characteristics in the turbulent and non-turbulent zones. In general it should exhibit a low or zero value in the non-turbulent flow and a finite, preferably much larger, value in the turbulent flow. However three major difficulties arise (Bradshaw & Murlis 1974). They are the physical difficulty that the interface is highly re-entrant (exhibiting deep short-duration penetrations of non-turbulent fluid), the mathematical difficulty that any function of velocity which is supposed to be non-zero within the turbulence will in fact have occasional zeros, and the operational difficulty that such a function may respond to high-wavenumber intermittency as well as interfacial intermittency. All three difficulties lead to the prediction of short non-turbulent regions within a turbulent 'burst': these are generally suppressed by the turbulence criterion functions adopted by most workers in this field, including the present authors. The criteria adopted by eleven authors are considered in detail by Bradshaw & Murlis with reference to the above discussion.

Reported measurements of this kind are far less common where the interface separates two turbulent flows. Clearly the difficulty of discrimination is much greater than in the simpler case of a turbulent/non-turbulent interface, unless an additional variable is introduced which will conform to the previously mentioned requirement that it should exhibit markedly different characteristics in each zone. An obvious choice is the application of heat to one of the two flows upstream of the interaction region and the detection of temperature thereafter as a basis for conditional sampling. Johnson (1959) did in fact apply a stepwise discontinuity in wall temperature to a turbulent boundary layer and reported intermittent temperature fluctuations at the interface between heated and unheated fluid. More recent authors who have used temperature intermittency include Charnay, Comte-Bellot & Mathieu (1972) in a boundary layer with free-stream turbulence, LaRue (1973) and LaRue & Libby (1974) in the turbulent wake of a heated rod and Antonia, Prabhu & Stephenson (1975) in an axisymmetric heated jet with a co-flowing stream. This technique of 'tagging' by temperature is emerging as a very effective method for analysing interacting flows, and so a fairly full account is given here.

In the present work, the lower boundary layer in the duct was heated by three lengths of nichrome resistance wire stretched across the wide end of the two-dimensional contraction about 3 cm from the floor, so that their heated wake emerged into the duct about 3 mm from the floor and mixed with the growing boundary layer long before the floor and roof boundary layers met (figure 1*b*).

Checks on the symmetry of $\overline{u^2}$ and $\overline{v^2}$ about the duct centre-line confirmed the absence of buoyancy effects. It was found that a fluid temperature rise of $\sim 3\,^{\circ}\mathrm{C}$ at station E (the region where the boundary layers begin to merge, at 26·5 duct heights downstream from the trip wire) provided adequate discrimination from the unheated layer as far as station J (57·0 duct heights; see figure 1). Thereafter, the cumulative effects of 'fine-grained' turbulent mixing undermined the effectiveness of the intermittency criteria: there is no reason in principle why the same techniques should not be used at these downstream stations, by uniformly heating the fluid in the lower half of the duct at, say, station H with a grid of fine heating wires normal to the flow.

One of the main difficulties in the conventional use of a hot wire is the effect of fluid temperature changes on the rate of heat transfer. Corrsin (1949) was probably the first author to express analytically the response of a hot wire to simultaneous velocity and temperature fluctuations. Using King's law, he derived the following expression for the instantaneous voltage fluctuations:

$$e = C_1\theta/T + C_2 u/U, \tag{1}$$

where θ and T are fluctuating and mean temperatures respectively and C_1 and C_2 are functions of the mean velocity calibration constants and of the hot-wire operating conditions. More recently, Bremhorst & Bullock (1970) derived a similar expression during measurements of temperature and velocity spectra in fully developed pipe flow. Wyngaard (1971) was mainly interested in the velocity sensitivity of a resistance-wire temperature sensor. In the present investigation, measurements of moments of the temperature fluctuations higher than θ^2 were not anticipated, allowing the neglect of velocity sensitivity in the light of Wyngaard's results: he showed that it would be negligible for most purposes, except for third and higher moments.

The response to fluid temperature of a hot wire operated at constant temperature can be readily obtained from a direct consideration of the definition of the Nusselt number, which is a measure of the heat transfer from the wire to the passing fluid:

$$Nu \propto \frac{E^2 T_w}{T_w - T_f}\frac{1}{K_f}, \tag{2}$$

where the subscripts w and f refer to wire and fluid respectively, and where we have assumed $R_w \propto T_w$. For there to be no temperature effect, Nu should not vary with T_f, the temperature of the fluid. The thermal conductivity of the fluid K_f is also dependent on T_f and, in common with the viscosity μ_f, it varies approximately as $T^{0.76}$. The fluid density is inversely proportional to temperature, so that the variations of Nu and $Re^{0.45}$ are very nearly the same, assuming that the same reference temperature is used for both. Thus, cancelling the temperature dependence of K_f and then evaluating the differential of Nu with respect to T_f yields the relation

$$e_\theta/E = -\tfrac{1}{2}\theta/(T_w - T_f), \tag{3}$$

where it is assumed that for small changes $dT_f \to \theta$ and $dE \to e_\theta$, which is the 'error voltage' in the instantaneous hot-wire output. In view of its simplicity,

(3) has been used throughout the present investigation to correct simultaneous measurements of fluctuating velocity, using the output from the temperature probe described below. It was found however that the generally small temperature difference between heated and unheated fluid produced less than 1% error in practically all the time-averaged turbulence quantities and no more than 10% in the remaining quantities, even when no correction was applied.

The instantaneous fluctuating temperature component was continuously recorded by a DISA 55F04 probe (with a 1 μm platinum wire) connected directly to a DISA anemometer operated in the constant-current mode without frequency compensation. The wire cut-off frequency (-3 dB point) was about 3 kHz, corresponding to a wavelength of about $0{\cdot}2h$: note that the threshold system of intermittency determination described in §4 implies that the more intense excursions of temperature will still be detected even at higher frequencies because the amplitude response falls as (frequency)$^{-1}$ at worst. The probe was mounted on the stem of a DISA miniature cross-wire probe within a wire's length of the cross-wires. There is no point in striving to reduce wire separation to less than a wire's length (1 mm) as this is the limit of spatial resolution. The idea of locating a temperature-sensitive probe close to a cross-wire probe is not new, although reports of previous investigations using this approach are few (e.g. Johnson 1959; Bremhorst & Bullock 1970; Bourke & Pulling 1970). The three-wire probe provided simultaneous records of velocity and temperature signals, which were recorded on analog magnetic tape (14 channel Ampex FR1300, frequency response 20 kHz at a tape speed of 60 in. s^{-1}). It was found that a recording of 6 s (real time) at each physical location in the flow was sufficient to provide adequate numerical convergence of the data. The analog recordings were digitized by the system then operating in the Aeronautics Department of Imperial College. This consisted of an IBM-compatible digital tape transport (Ampex TM16) fed by a DEC AD08B Analog-to-Digital converter with sample-and-hold and provision for up to 16 multiplexed channels (4 implemented) indexed under RC clock control. The AD output was read into the accumulator of a PDP 8/L minicomputer by a software service routine and deposited in two temporary buffers each of 1536 words (3000_8) in the core. The buffer not being currently filled by the AD was read out in 'cycle-stealing' mode to the tape transport and written on 7-track $\frac{1}{2}$ in. magnetic tape for subsequent analysis on the main Imperial College computer (CDC 6400). The full details of this system and of the program CS4-A, which carried out the statistical analysis of the digitized signals on the main computer, are explained by Dean (1974*a*) and Brandt & Bradshaw (1972) and some recent improvements are described by Weir & Bradshaw (1974). A useful guide to the terminology used in analog-to-digital conversion work is given by Gibson (1973). The intermittency criteria were originally developed by Dean in liaison with Brandt. They are non-trivial and are explained in the next section.

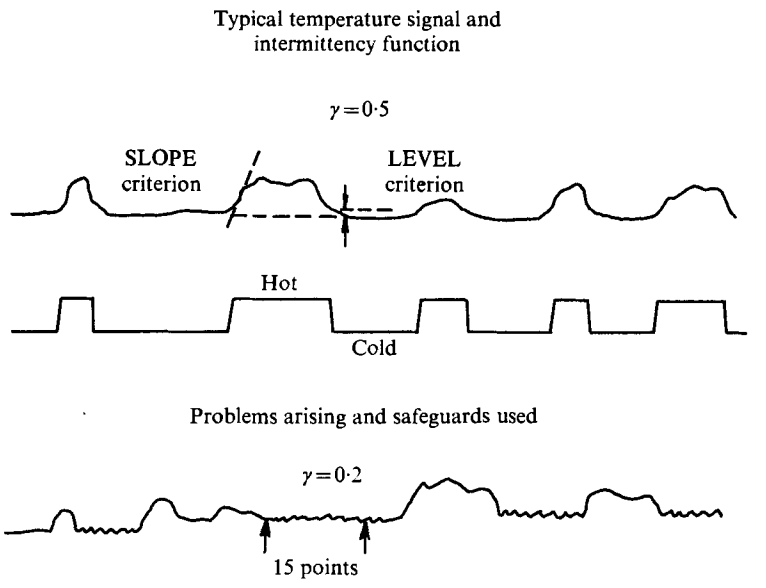

FIGURE 2. Intermittency criteria and safeguards used.

4. Temperature-intermittency criteria

Since the temperature probe will not respond to fluctuations of wavelength much less than $0{\cdot}2h$, any fine-structure in the temperature intermittency is automatically smoothed out. Bradshaw & Murlis (1974) distinguish 'retail' and 'wholesale' intermittency measurements as those that respectively do or do not resolve the fine-scale corrugations of the intermittency interface. Thus the intermittency values given below are 'wholesale', like most previous measurements of velocity or temperature intermittency.

Inspection of temperature traces indicated that the 'hot' bursts were of varying amplitude and took place in the presence of low frequency ($\sim$ 130 Hz) temperature undulations of extraneous origin, presumably present in the room air before it enters the blower. Clearly a simple magnitude criterion will not suffice to identify a 'hot' region and a general intermittency procedure of this type, which could be applicable to a wide range of flows, should be able to allow for both these effects. It is interesting to note, however, that both LaRue (1973) and Antonia (1974) have used just the one magnitude criterion (threshold level) without reference to the above difficulties. In the present investigation, it was decided that it would be more expedient to measure the first derivative of the temperature signal at each point, hereafter called the SLOPE. This is obtained as a central difference, from the preceding and succeeding values of the digitized instantaneous temperature voltage. To allow for the slowly varying mean value observed in the 'cold' signal, a LEVEL criterion was adopted which would only be tested at each point if the SLOPE was less than the prescribed limit. Numerical

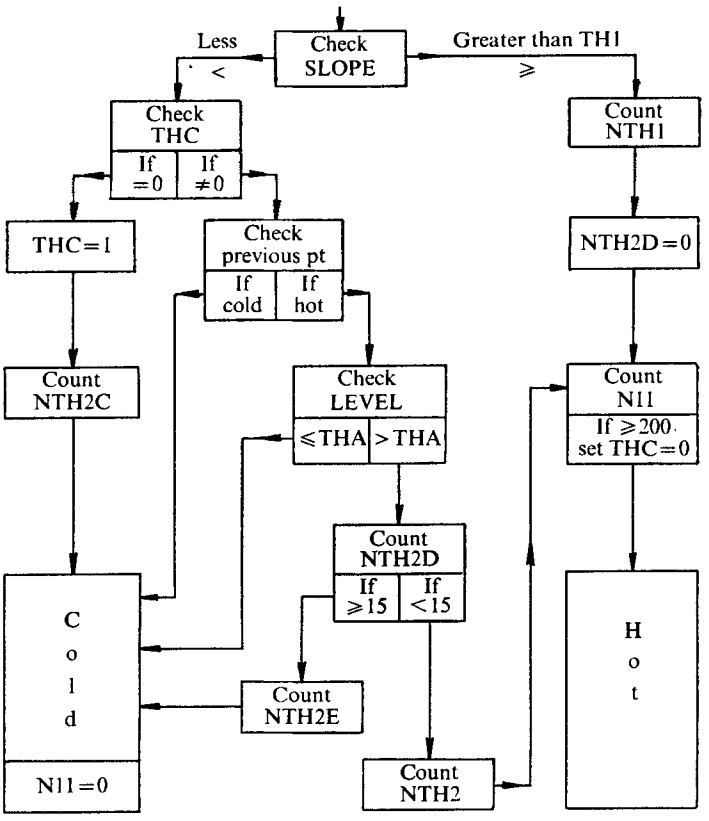

FIGURE 3. Intermittency flow chart.

values for these criteria were chosen by inspection of Calcomp plots and were labelled as TH1 (SLOPE) and TH2 (LEVEL) within the program. The sensitivity of the intermittency factor γ to the threshold levels was similar to that usually found in measurements of velocity-field intermittency: near $\gamma = 0{\cdot}5$, say, a given percentage change in TH2 changed γ by a percentage which was significantly smaller but not an order of magnitude smaller, as can be inferred from the sketch in figure 2.

Each of the two criteria is shown in figure 2 applied to a typical temperature signal of intermittency $\gamma \approx 0{\cdot}5$. The LEVEL criterion THA is in fact a distance TH2 above the ambient 'cold' level: at the beginning of each 'hot' burst, the current 'cold' level is stored and, as soon as the SLOPE at any point in the burst is less than TH1, that point is called 'cold', unless its magnitude is greater than the stored level plus TH2. (The real time interval between each point is $\frac{1}{2} \times 10^{-4}$ s or $\overline{U}t/h = 0{\cdot}03$ or about one temperature-probe time constant.) In this way, each 'hot' burst is given individual treatment using a self-adjusting LEVEL criterion. One initial difficulty did arise using this technique: occasionally during a 'hot' burst, the slowly varying 'cold' level suffered a permanent change which exceeded the sum of the current level (at the start of the burst) and TH2. This is shown in the lower sketch in figure 2 for a temperature signal with low inter-

mittency ($\gamma = 0{\cdot}2$). The 'cold' regions in this example have been deliberately drawn so as to illustrate the maximum noise level in any of the signals obtained. A 'hot' burst is shown which is apparently about 5 points in length but which clearly does not return to within TH2 of the initial 'cold' level, even after a further 15 points, owing to a sudden rise in the ambient level. If this failure is not remedied, then the remainder of the digital recording will be called 'hot' until the LEVEL criterion is eventually satisfied, if at all. A large number of Calcomp plots showing signals of low intermittency were checked and it was found that 'hot' bursts containing only points of low SLOPE (i.e. flat-topped ones) never exceeded 15 points in length. A 'safeguard' was therefore introduced into THRESH which counts 'hot' points of low SLOPE. Thus when 15 consecutive 'hot' points of low SLOPE ($<$ TH1) have been counted, the current point is called 'cold' and the 'hot' burst is terminated. The next point is tested in the usual way. A rather similar problem arises for signals with high values of γ; a sudden rise in the ambient 'cold' level might again produce an all 'hot' intermittency function. It was found from Calcomp plots that the maximum continuous 'hot' burst rarely exceeded 200 points (burst length $\approx 6h$). This number was counted by THRESH and a limit of 200 set for the present group of recordings. Thus, when 200 consecutive 'hot' points of any SLOPE have been counted, the next point with SLOPE $<$ TH1 is immediately called 'cold' and the 'hot' burst is terminated. The succeeding point is tested in the usual way. It should be emphasized that both these events are rare.

The procedure is summarized in figure 3. At each point the SLOPE is checked: if it is greater than or equal to the criterion value TH1, the point is automatically called 'hot'. The total number of 'hot' points discriminated directly by the SLOPE test is counted in NTH1 and the check NTH2D on consecutive 'hot' points of low SLOPE is set to zero. The total number of consecutive 'hot' points is stored in N11 and, if the current point is the 200th, then the check THC is set to zero and the next point with SLOPE $<$ TH1 will immediately be called 'cold'. If the current point has a SLOPE less than the criterion value TH1, then THC is initially checked for the 200-point safeguard. The number of times this is used is recorded in NTH2C. If THC is non-zero (i.e. N11 $<$ 200), the previous data point is checked. If it was 'cold', then the present one cannot be 'hot' (a 'hot' burst cannot begin with a low SLOPE) and it is therefore called 'cold'. If it was 'hot', the LEVEL criterion is tested and, if the signal has returned to within TH2 of its value at the beginning of the 'hot' burst, that point is called 'cold'. If not, it may be one of 15 consecutive 'hot' points of low SLOPE. If NTH2D $<$ 15, the point is called 'cold' and the use of the 15-point safeguard is registered in NTH2E. If NTH2D $<$ 15, the point is finally called 'hot' and N11 is incremented accordingly. The number of points eventually called 'hot' after passing these tests is recorded in NTH2.

Although this algorithm worked well on the present data (i.e. the computed intermittency function agrees well with that drawn by eye for the same temperature trace), Weir & Andreopoulos (private communication) found that it failed to give acceptable results in similar investigations of interacting free shear layers, because of the presence of long bursts of hot fluid with $\partial\theta/\partial t$ no greater than in

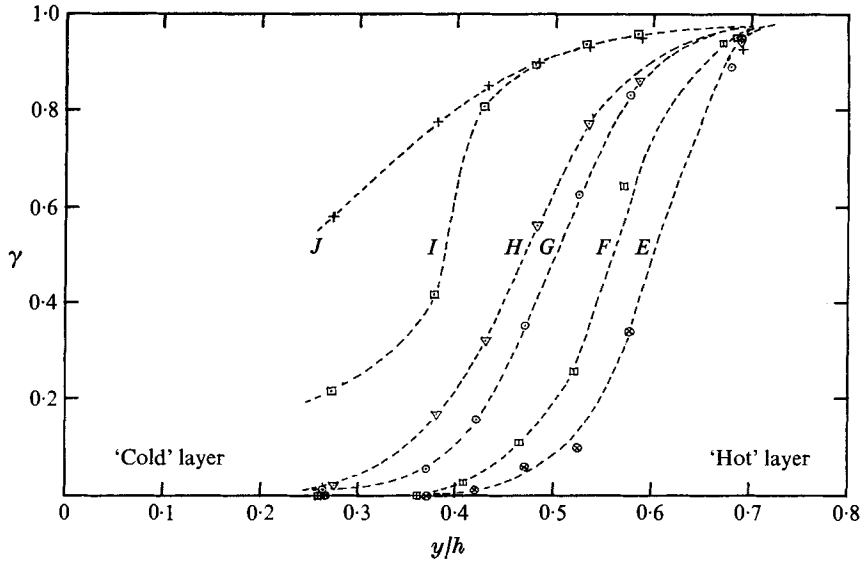

FIGURE 4. Intermittency profiles at stations *E*–*J*.
- - -, approximate mean line through data.

	⊗	◫	⊙	▽	⊡	+
Station	*E*	*F*	*G*	*H*	*I*	*J*
x/*h*	26·5	32·6	38·7	44·8	50·9	57·0

the nearly cold fluid. They therefore used an algorithm based primarily on level, but with slope as a back-up criterion to avoid the problem illustrated in figure 2 (*b*).

Figure 4 shows the family of intermittency profiles obtained at stations *E*–*J* when heat was applied to the lower boundary layer. At stations *I* and *J*, examination of temperature traces shows that, because of the cumulative effect of fine-scale mixing near the centre-line, the 'hot' and 'cold' zones become so small and frequent that the intermittency technique becomes unreliable. Thus the point in the flow where $\gamma = 0{\cdot}5$ moves steadily towards $y = 0$ with increasing distance downstream, owing to heating of the 'cold' fluid by the 'hot' layer in a region near the centre-line. If there were no heat loss to the walls of the duct, the temperature would eventually become uniform. Quantitative values for burst length are not presented here. At the time that the work was done we were aware of the inherent difficulty in defining an 'average burst length' (for instance, the average burst length is halved if each burst contains a very short drop-out near mid-length) but did not have the probability-distribution analysis of Murlis (1975), which goes some way towards resolving the difficulty.

The conditionally sampled turbulence quantities have been calculated by measuring fluctuations about the conventional mean velocity, in contrast to the scheme, used by Hedley & Keffer (1974) and others, in which fluctuations in the 'turbulent' region are measured with respect to the regional-average velocity. The difference is explained in figure 5, where it can be seen that a common baseline permits application of the addition law

$$\gamma \bar{Q}_{\mathrm{HOT}} + (1-\gamma)\,\bar{Q}_{\mathrm{COLD}} = \bar{Q}_{\mathrm{TOTAL}} \qquad (4)$$

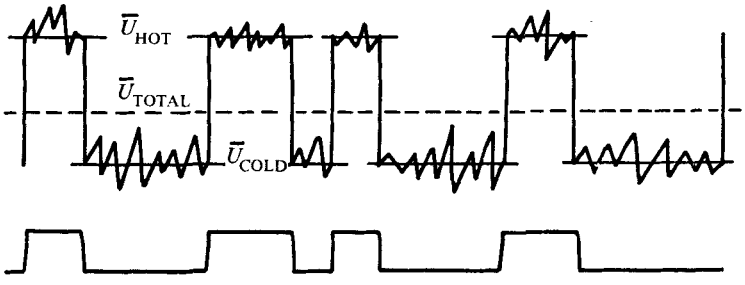

'Regional' baseline: $U_{HOT} = \overline{U}_{HOT} + u_{HOT}$ *a*

'Total' baseline: $U_{HOT} = \overline{U}_{TOTAL} + u_{HOT}$ *b*

b Enables addition law to be applied:

$\gamma\ \overline{Q}_{HOT} + (1-\gamma)\overline{Q}_{COLD} = \overline{Q}_{TOTAL}$ *c*

e.g. $\gamma\ \overline{uv}_{HOT}$ = 'hot' contribution to $\overline{uv}_{TOTAL}$

$(1-\gamma)\overline{uv}_{COLD}$ = 'cold' contribution to $\overline{uv}_{TOTAL}$

FIGURE 5. Choice of baseline.

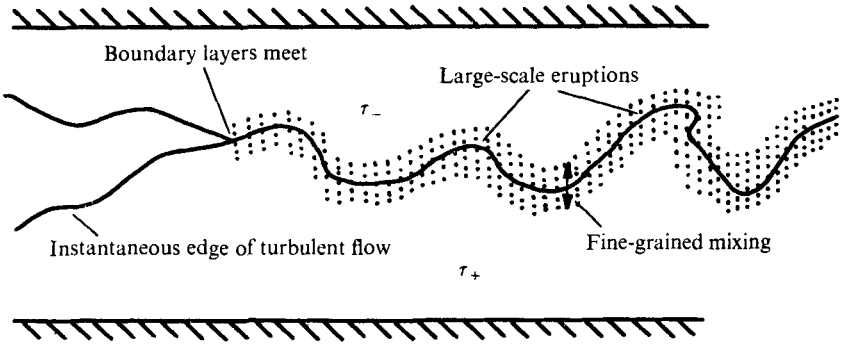

FIGURE 6. Postulated behaviour of interacting shear layers.

to products like $\overline{u^m v^n}$ for $m, n = 0, 1, 2$, though *not* to $\overline{u^m}/\overline{v^n}$. One must distinguish carefully between the average within the hot fluid, $\overline{Q}_{HOT}$, hereafter abbreviated to $\overline{Q}_H$, and the contribution of the hot fluid to the conventional average $\overline{Q}_{TOTAL}$ (hereafter abbreviated to $\overline{Q}$), which is $\gamma\overline{Q}_H$. Most of the results below are presented in the latter form. It is conceptually easier to discuss results which satisfy (4): the use of regional averages as a baseline for fluctuation measurements ignores the fact that the difference between regional-average and conventional-average velocity is the main contribution of the *large* eddies to the conventional-average turbulence intensity. In the present case, a common baseline permits an assessment of the contribution that the turbulence fields of each shear layer make to the total turbulence at any point in the flow.

5. Overlap of the shear layers

It has long been realized that the flow in a duct does not reach a state of full development (where the mean and turbulent properties are invariant in the flow direction) until long after the boundary layers have met, although the exact

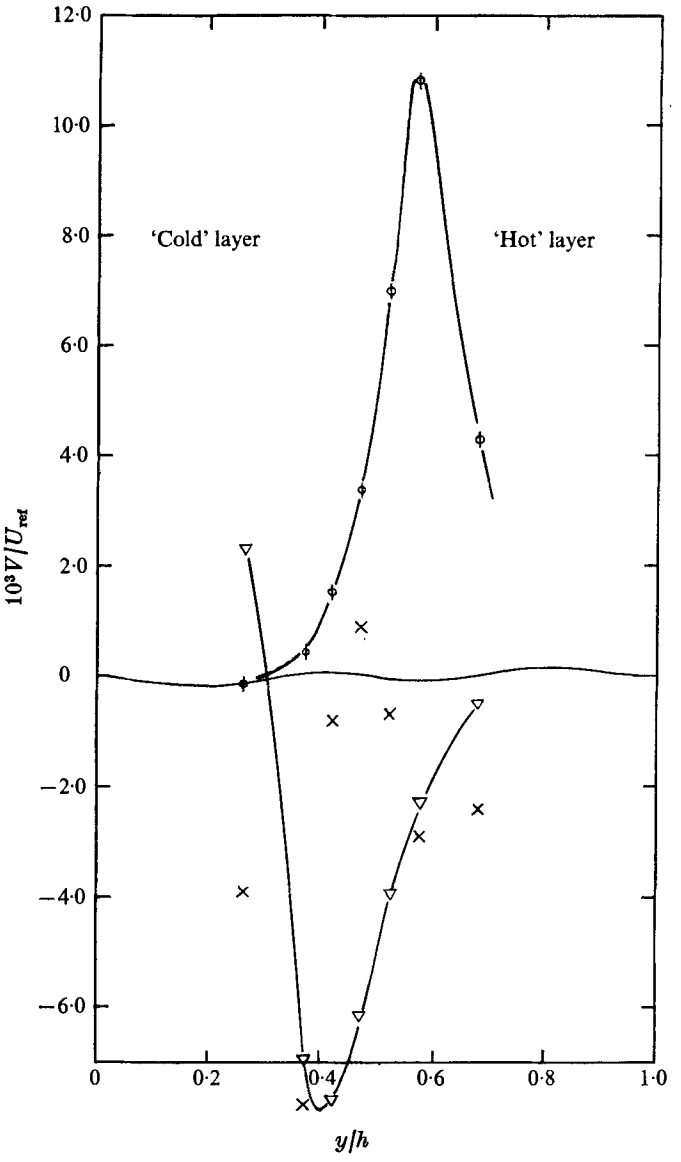

FIGURE 7. Mean V at station G, $x/h = 38{\cdot}7$. Results *not* multiplied by γ. ∇, hot-zone average; ϕ, cold-zone average; ——, conventional-average prediction (Bradshaw *et al.* 1973); $\times$, uncorrected conventional-average measurement.

location of full development is still debated (perhaps fruitlessly, since it is an asymptotic state). It has also been observed that the centre-line velocity continues to increase for about 15 duct heights after the layers have begun to merge before decreasing to its final value. The velocity profile shape parameter also 'overshoots'. None of the several investigators who have reported this overshoot (e.g. Reichert & Azad 1976) have offered a convincing explanation and some thought it a curious and significant phenomenon. Therefore it seems worthwhile to give a simple explanation before discussing the details of shear-layer inter-

action. The cause of the overshoot is the nonlinear shape of the shear-stress profile just after boundary layers meet: $\partial\tau/\partial y$ near the centre-line is smaller than dp/dx and so the flow continues to accelerate. The shear-stress profiles continue to merge and $\partial\tau/\partial y$ exceeds dp/dx: the centre-line velocity therefore decreases until the shear-stress profile collapses back to the familiar linear shape. The turbulence field appears to respond in the same way with centre-line values of $\overline{u^2}$, $\overline{v^2}$, $\overline{u^2v}$ and $\overline{v^2u}$ reaching their maxima after the boundary layers have merged and then falling towards their fully developed values. These are the outward signs of interaction but qualitative examination of profiles does not demonstrate the extent of the interaction: changes in profile shape could be explained by pure superposition of the two turbulence fields. Indeed, the prediction method of Bradshaw *et al.* (1973) allows interaction through the mean velocity profile only and the good fit to experimental data (including the reproduction of the 'overshoot' discussed above) suggests that, at least for purposes of modelling the shear-stress transport equations, the shear layers can be said to overlap without any interaction in the sense of disturbance of the turbulence structure.

When the layers begin to merge, the outer-layer eddies, which produce the familiar convoluted edge to the boundary layer, continue to erupt but are now erupting into the turbulent flow field of the other shear layer rather than an irrotational free stream. Figure 6 shows the postulated behaviour of the interacting shear layers. Note that only the 'wholesale' eruptions are shown: each eruption probably has associated smaller-scale convolutions of the interface, as in a boundary layer below a non-turbulent stream (Bradshaw & Murlis 1974). Although fluid with positive shear stress will be intruding into a region of negative $\partial U/\partial y$ (and vice versa), there is no reason to suppose that the length scale of this process will be diminished, as long as the interaction is weak. A measure of the momentum that these intruding eddies possess can be deduced by reference to the profiles of the normal component V of conditional-mean velocity. These were plotted with respect to the TOTAL (conventional-average) values predicted by the calculation method of Bradshaw *et al.* (1973). These were used instead of measured values simply to provide a smoother zero datum to facilitate observation of the 'hot' and 'cold' contributions to V (it is impossible to measure V to good percentage accuracy with a hot-wire anemometer, unlike $\overline{v^2}$ and the higher moments of v, which are calculated from the difference between the instantaneous vector and its mean value). It was found that at stations *G*–*J* the value of V in the cold fluid, V_C, always reached a maximum at $y/h \simeq 0{\cdot}6$, indicating that the mean position where the intruding eddies from both sides of the duct erupt most vigorously is about $\pm 0{\cdot}1h$ from the centre-line. As an example, the data at station *G* are shown in figure 7: $V_H(y)$ is nominally equal to $V_C(h-y)$. This result suggests that, although the strength of the interaction undoubtedly increases as the boundary layers merge, its limit of spread towards the wall is confined to a small region near the duct centre-line. Furthermore, this appears to confirm that the curious shape of the γ profiles at *I* and *J* in figure 4 is entirely due to fine-scale mixing and consequent breakdown of the intermittency criteria, and does not indicate continuing penetration of each shear layer by the other towards the wall. The consistency of the intermittency measurements up to

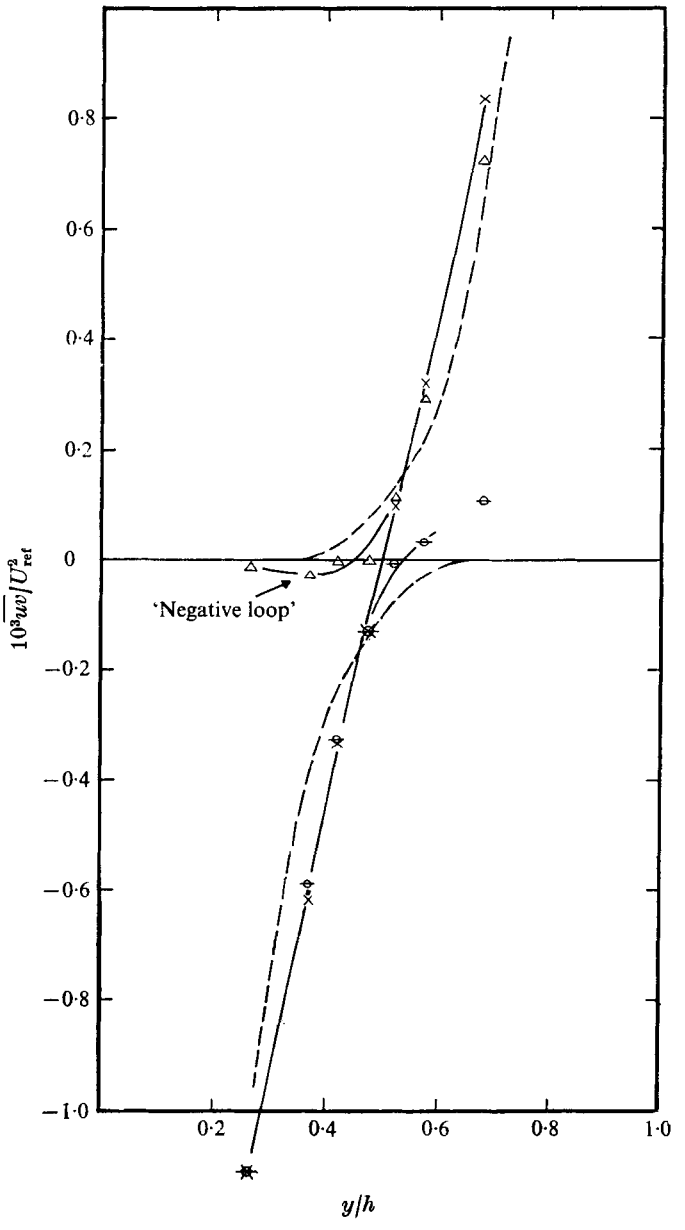

FIGURE 8. $\overline{uv}$ at G, $x/h = 38{\cdot}7$. ×, conventional-average $\overline{uv}$; △, hot-zone contribution to conventional average, $\gamma\overline{uv}_H$; ⊖ cold-zone contribution to conventional average, $(1-\gamma)\,\overline{uv}_C$; — — —, conventional-average production (Bradshaw *et al.* 1973).

station H is itself evidence in favour of the mild form of interaction postulated in figure 6. The intermittency itself is not constrained by symmetry requirements, but, at any station, the 'hot' and 'cold' contributions to turbulence quantities should be symmetrical about the duct centre-line $y/h = 0{\cdot}5$ (with a change of sign in the case of odd functions). Failure to satisfy these requirements (e.g. the

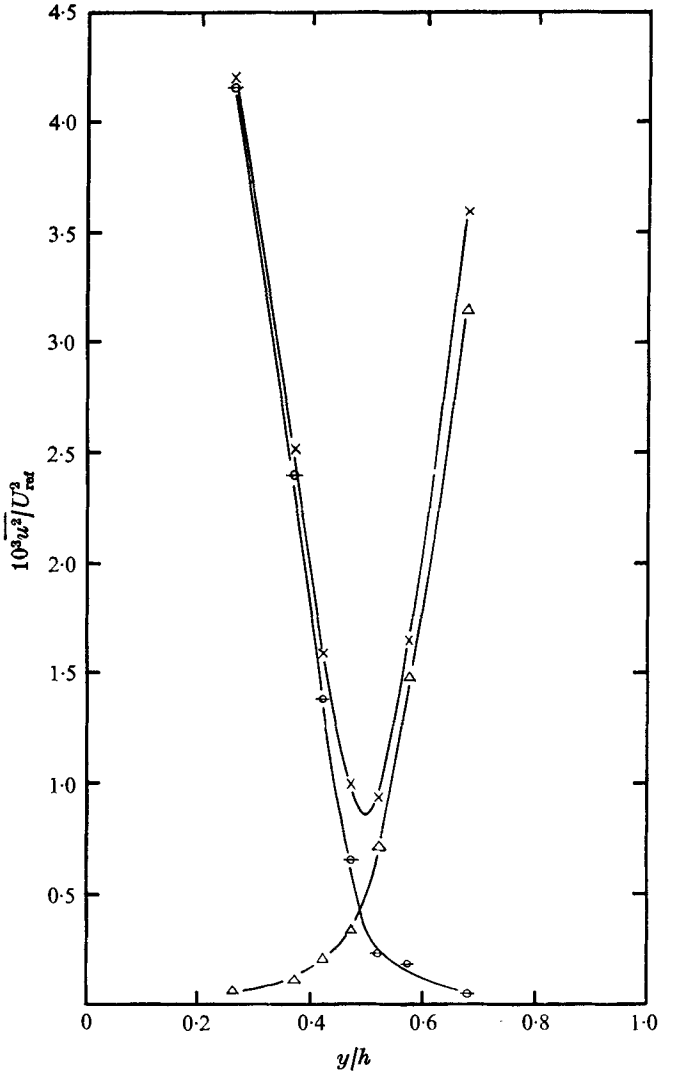

FIGURE 9. $\overline{u^2}$ at G, x/h = 38·7. Notation as in figure 8.

slight asymmetries in figures 9 and 10) implies measurement errors, principally in the intermittency.

Plots of the conditionally averaged shear stress revealed that the 'hot' and 'cold' components ($\gamma\overline{uv}_H$ and $(1-\gamma)\overline{uv}_C$ respectively) of $\overline{uv}$ asymptote to zero quite rapidly near the duct centre-line (the plot for station G is given in figure 8 as an example), showing less overlap than was predicted by Bradshaw *et al.* (1973). In addition, the 'hot' and 'cold' $\overline{uv}$ profiles at stations F–H (the first three stations after the boundary layers meet) show a non-monotonic approach to zero, hereafter called a 'negative loop', as well as the expected overlap. This effect may be clearly seen in figure 8: intermittency errors are not likely to be wholly responsible and several explanations must be considered. For example,

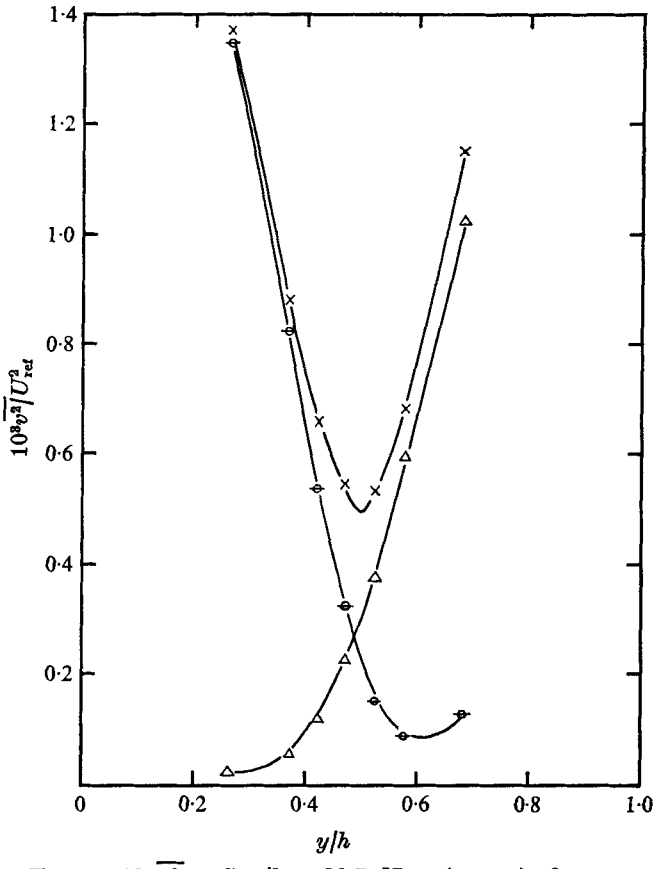

FIGURE 10. $\overline{v^2}$ at G, $x/h = 38{\cdot}7$. Notation as in figure 8.

it could be argued that 'cold' fluid entrained by the 'hot' layer is rapidly heated before the host layer has time to impose its own turbulence structure, so that, if it becomes part of any eddy erupting into the 'cold' layer, the intermittency criteria label it as 'hot' fluid with negative uv (instead of positive). Alternatively, 'hot' fluid intruding into the 'cold' layer may be rapidly sheared before any noticeable cooling takes place. It seems far more likely that cooling and shear-stress reversal both occur at the same rate and are anyway closely related in a fine-scale mixing process which takes place around the boundaries of the large erupting eddies: as the fluctuating strain $\partial u/\partial y$ has a zero mean value, the shearing of (say) 'hot' fluid by 'cold' turbulence will not have much net effect until the 'hot' fluid is well mixed in. Furthermore, the time taken by the mean strain $\partial U/\partial y$ to reduce the turbulence intensity

$$\tau \simeq \frac{\frac{1}{2}\overline{q_{\mathrm{H}}^2}}{-\overline{uv}_{\mathrm{H}}\,\partial U/\partial y} \tag{5}$$

of the erupting fluid is $\simeq 7h/\overline{U}$ at station G, which would be far too long. The maximum point in the negative loop of 'hot' and 'cold' $\overline{uv}$ at all stations (E–J) was found to be at roughly $\pm 0{\cdot}1h$ from the centre-line where it had previously been observed that the eddies would be erupting most vigorously.

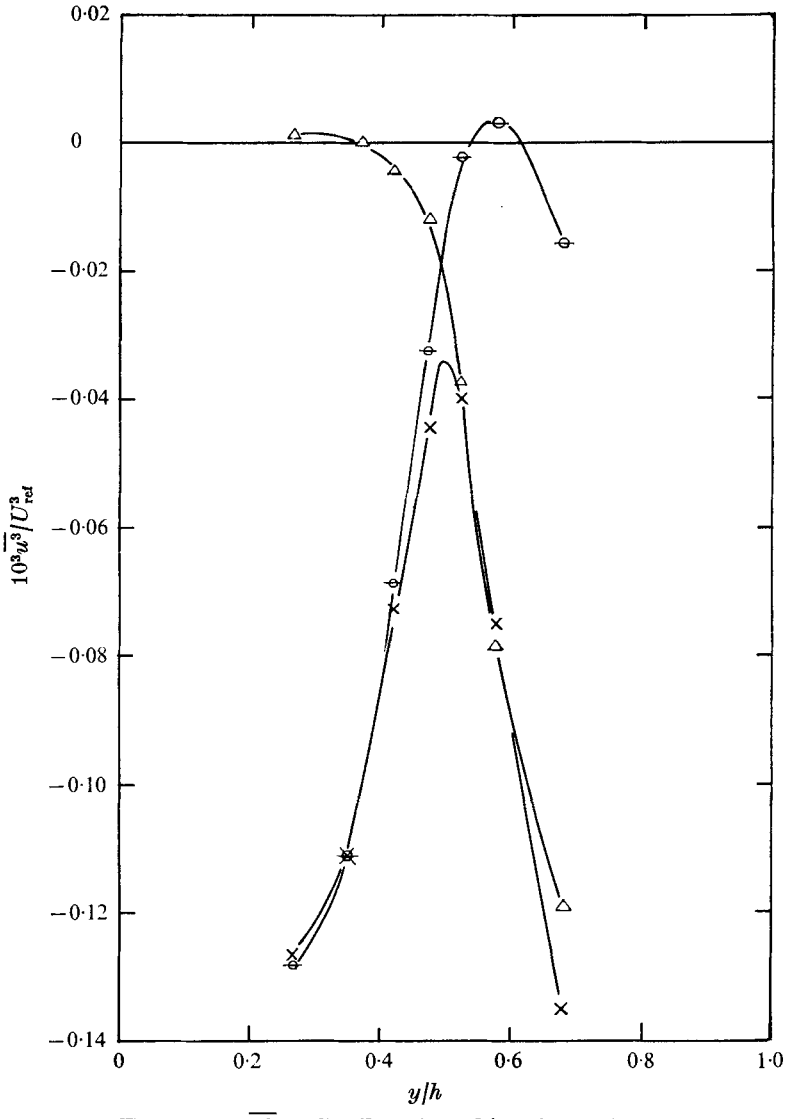

FIGURE 11. $\overline{u^3}$ at G, $x/h = 38{\cdot}7$. Notation as in figure 8.

Further insight into the interaction and the effects of negative $\partial U/\partial y$ can be gained by considering the overlap of the 'hot' and 'cold' profiles of other turbulent quantities (figures 8–14). It is important to note that these figures do not themselves provide conclusive evidence for or against the superposition ('time-sharing') hypothesis; even if that hypothesis were true, the hot-zone intensity profiles would still differ from those of an ordinary boundary layer because the mean velocity gradient in the 'free stream' (the cold half of the duct) is non-zero. To test the superposition hypothesis we examine, in §6, the dimensionless structural parameters of the hot-zone turbulence and compare them with measurements in boundary layers. In order of increasing overlap, the second- and

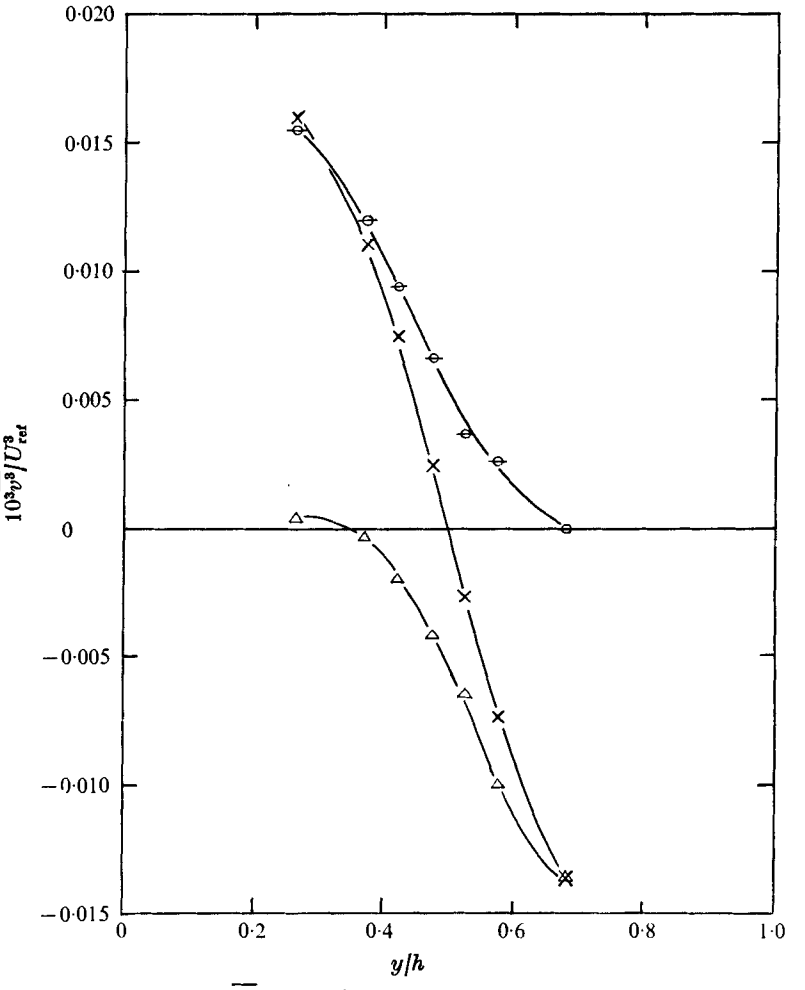

FIGURE 12. $\overline{v^3}$ at G, $x/h = 38{\cdot}7$. Notation as in figure 8.

third-order mean products are $\underline{\underline{uv}}$, $\overline{u^3}$, $\underline{\underline{uv^2}}$, $\overline{u^2v}$, $\overline{u^4}$, $\overline{v^2}$, $\underline{\underline{v^3}}$, $\overline{v^4}$ and $\overline{u^2}$. In the case of the antisymmetric functions, underlined above, the order of increasing overlap is also the order of *decreasing* negative loops. From the discussion of $\overline{uv}$, it is not surprising that the extent of overlap of 'hot' and 'cold' $\overline{u^2}$ and $\overline{v^2}$ is quite significant and in fact greater in the case of $\overline{u^2}$ than for any of the other turbulence quantities reported here (e.g. figures 9 and 10). In the duct prediction method of Bradshaw *et al.* (1973) it is assumed that the turbulent energy $\overline{q^2}$ is directly proportional to the local mean shear stress. Comparison of the extents of overlap of the intensity and shear-stress profiles suggests that $\overline{q^2}$ overlaps slightly *more* than is predicted by the program, while $\overline{uv}$ overlaps less.

The triple products $\overline{u_iu_ju_k}$ are in general non-zero and represent the transport of the quantity $\overline{u_iu_j}$ by the convective action of the velocity fluctuation u_k. The derivative of $\overline{u_iu_ju_k}$ with respect to x_k appears in the transport equations for the

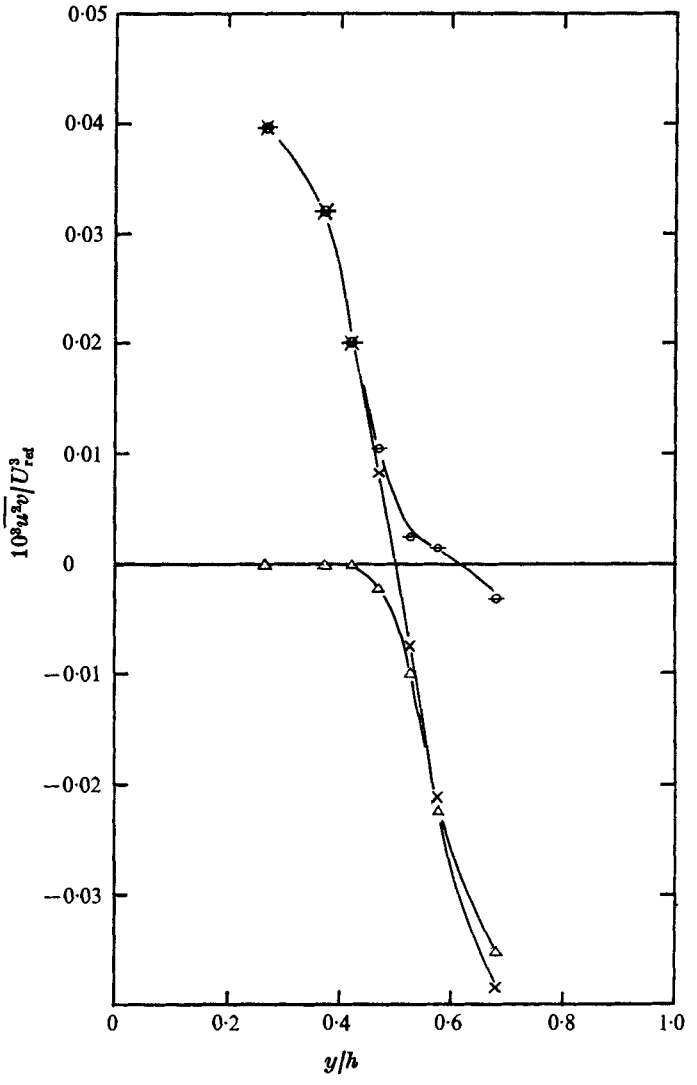

FIGURE 13. $\overline{u^2v}$ at G, $x/h = 38{\cdot}7$. Notation as in figure 8.

turbulent stresses as part of the turbulent diffusion term and also in the turbulent energy equation in the diffusion term in the less general form $\overline{u_i^2 u_k}$. At the edge of a boundary layer, high longitudinal intensity is transferred by negative fluctuating components of u, resulting in negative values of $\overline{u^3}$. Thus, when an eddy erupts into a region of negative mean strain $\partial U/\partial y$, the effective u becomes less negative and $\overline{u^3}$ within the intruding fluid will rapidly decrease with distance either side of the centre-line (figure 11). The quantity $\overline{v^3}$, in contrast to $\overline{u^3}$, was found to be significant in fluid which has erupted across the centre-line (e.g. figure 12). No negative loop could be detected at stations downstream of E; had there been any, it could have been interpreted as evidence that the intruding eddies were

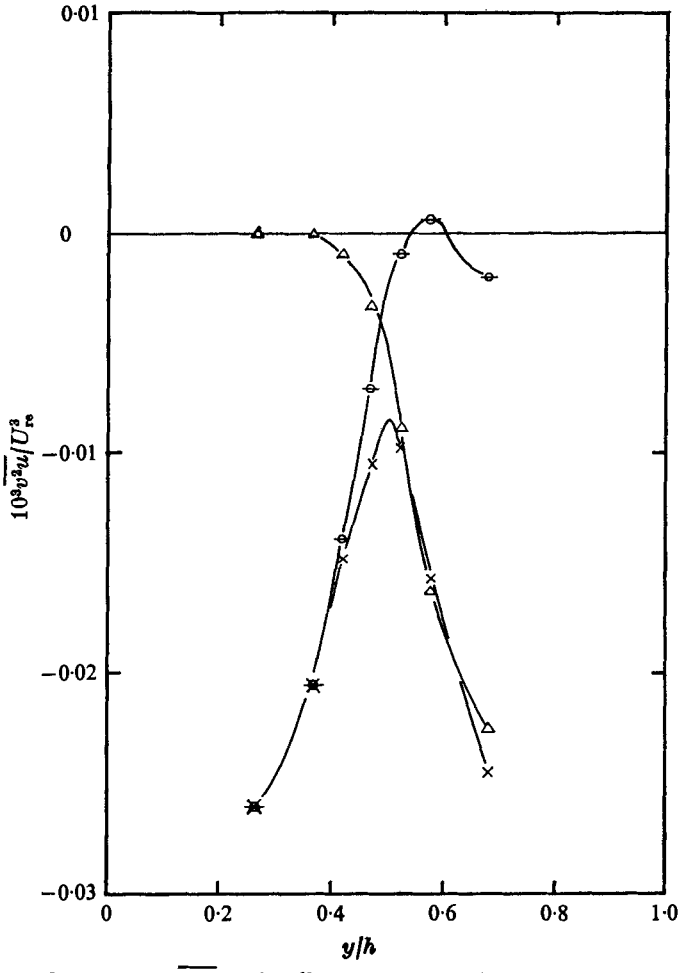

FIGURE 14. $\overline{v^2u}$ at G, $x/h = 38{\cdot}7$. Notation as in figure 8.

actually being pushed back into the shear layer from which they had originated, contrary to the idea of superposition. Rather less overlap was observed in $\overline{u^2v}$ and $\overline{v^2u}$ (e.g. figures 13 and 14 respectively), again without a negative loop. The diffusion of turbulent energy, in the eddies erupting across the centre-line, therefore seems to be dominated by $\overline{v^3}$, the transfer of normal turbulence intensity by the normal fluctuating component of velocity. This component is similarly responsible for the transfer of shear stress in $\overline{v^2u}$, whose small extent of overlap indicates rapid attenuation of the turbulent diffusion of shear stress, commensurate with the process of entrainment and subsequent reversal of the shear stress of the intruding fluid. This supports the general analogy with the outer layer of a single boundary layer, in which Phillips' (1955) theory demonstrates that the irrotational motion is mainly forced by the v component.

Overlap in $\overline{v^4}$ was apparently very high, being surpassed only by $\overline{u^2}$, whilst $\overline{u^4}$ exhibited roughly the same amount as $\overline{v^2}$. Time-averaged quadruple products are

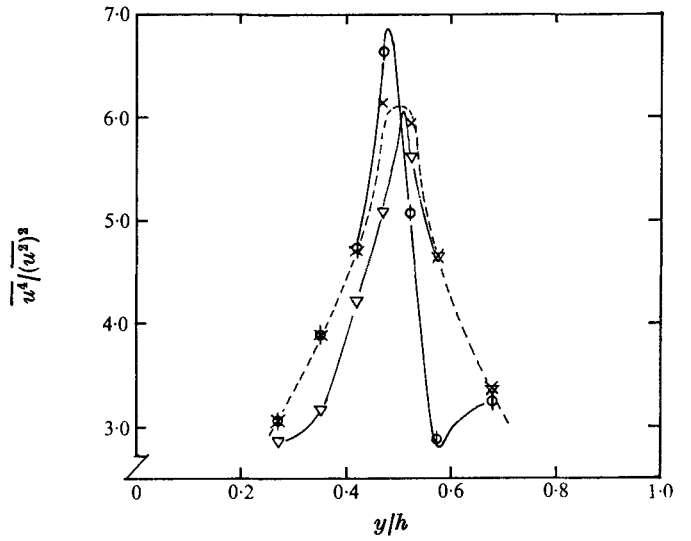

FIGURE 15. u flatness factor at G, $x/h = 38{\cdot}7$. ×, conventional average; ▽, hot-zone average; ϕ, cold-zone average. Results not multiplied by γ.

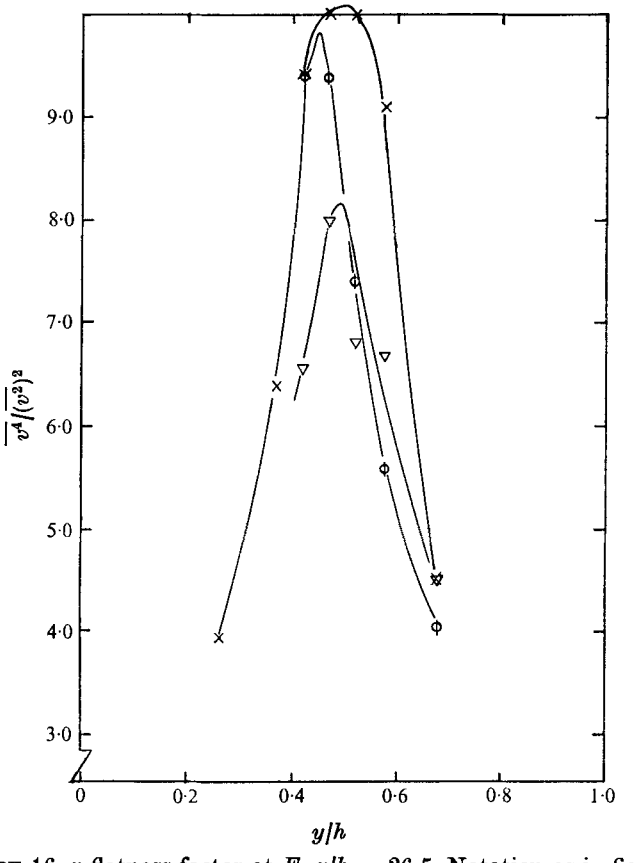

FIGURE 16. v flatness factor at E, $x/h = 26{\cdot}5$. Notation as in figure 15.

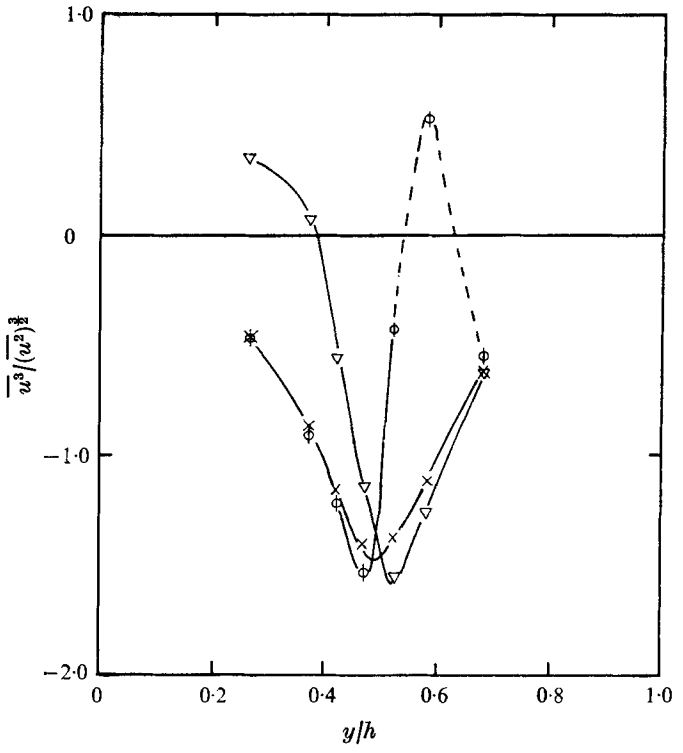

FIGURE 17. u skewness at G, $x/h = 38{\cdot}7$. Notation as in figure 15.

strongly affected by occasional large amplitude bursts of turbulence and are therefore useful for indicating the existence of intermittent flows. Non-dimensionalized by the square of the local mean-square intensity, these quantities become the flatness factors $\overline{u^4}/(\overline{u^2})^2$ and $\overline{v^4}/(\overline{v^2})^2$ for u and v respectively. The complete set of profiles for conditionally sampled measurements of u and v flatness and skewness at stations E–J is given by Dean (1974*a*) while the data obtained at G are shown in figures 15–18. The 'hot' and 'cold' contributions have not been multiplied by γ and $1-\gamma$ because flatness or skewness, being made dimensionless by conditionally sampled quantities, do not obey an equation like (4): in any case, the physical meaning of the factors is best assessed for 'hot' and 'cold' regions independently, so that multiplication by γ or $1-\gamma$ is again inappropriate. As evaluated with respect to the total baseline, the factors represent the statistics of excursions from the mean velocity rather than the variability of excursions about the average 'hot' or 'cold' excursion. In a Gaussian process, the u skewness would be zero but on the duct centre-line there are negative contributions from both layers: the total v skewness is zero by symmetry. The results for u and v skewness (e.g. figures 17 and 18) essentially confirm the physical arguments of the previous paragraphs. The u skewness of 'hot' fluid intruding into the 'cold' layer (the region of negative $\partial U/\partial y$) exhibits a rapid reduction with distance from the centre-line, falling to zero near $y/h = 0{\cdot}4$. It is probably fortuitous that this position coincides with a u flatness of about 3 at the same

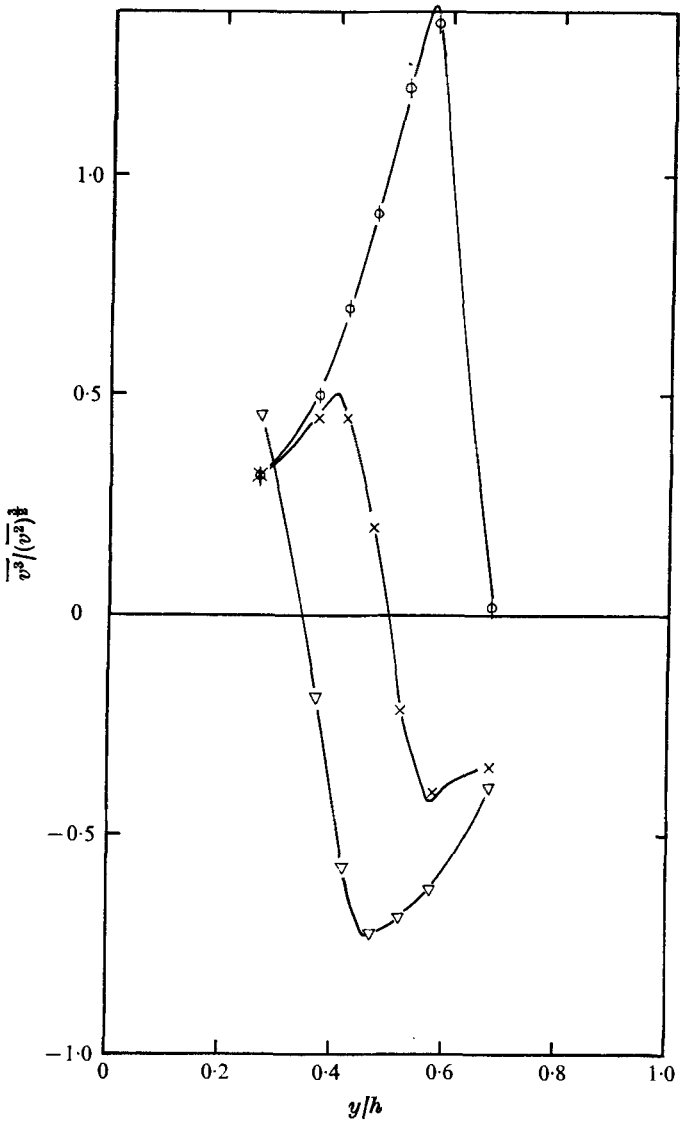

FIGURE 18. v skewness at G, $x/h = 38{\cdot}7$. Notation as in fig. 15.

stations. Furthermore the total v skewness reaches extrema of opposite signs at $\pm 0{\cdot}1h$ either side of the duct centre-line after passing through zero at $y/h = 0{\cdot}5$, whilst the zone averages of opposite sign to the total fall to zero at nearly the same rate. It has been mentioned that high flatness factors may be associated with intermittent flows, and in figure 19 it can be seen how the profiles of conventional u flatness (total ensemble averages) collapse to the fully developed state at station P ($x/h = 93{\cdot}6$), indicating a final centre-line value of 3·73. Values of the v flatness were found to exhibit a similar collapse with a centre-line value of 3·8 at station J (v flatness was not measured at station P). These values would be obtained if the flow near the centre-line consisted of bursts with a Gaussian

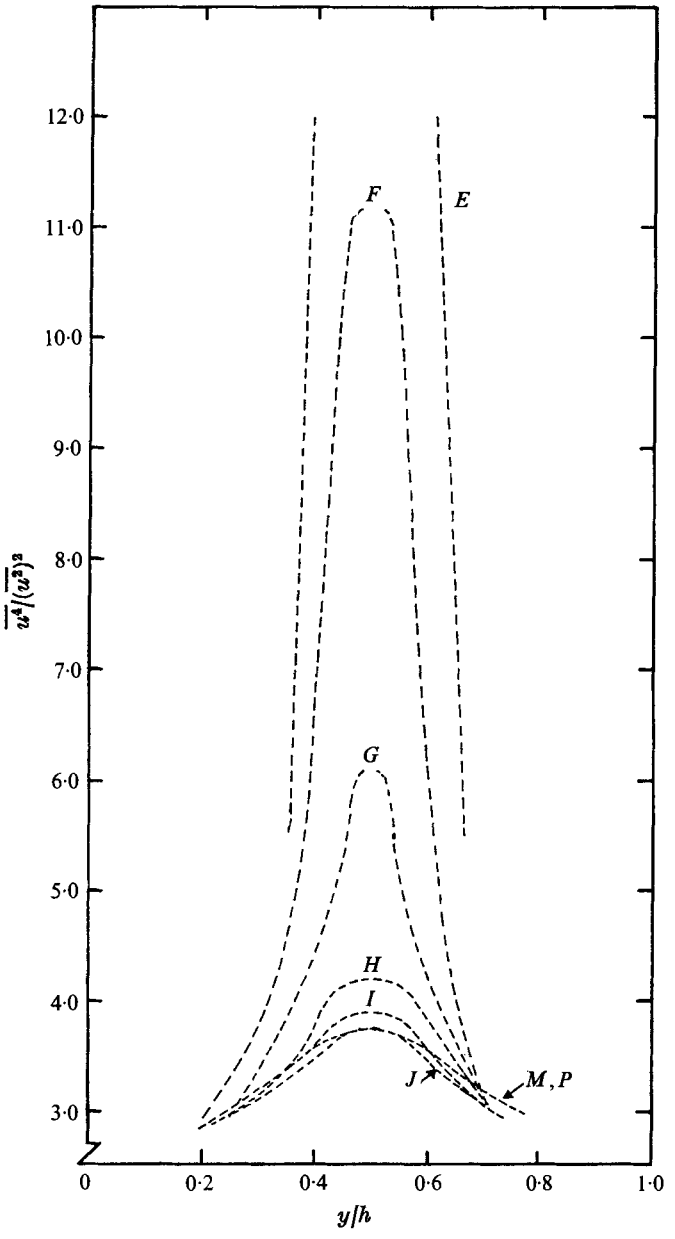

FIGURE 19. u flatness factor development, stations E–P: conventional averages.

probability distribution (flatness factor 3) occupying about 0·8 of the total time, with quiescent intervals occupying 0·2 of the total time. The flow behaviour postulated in figure 6, with bursts alternating with low-intensity fine-grained mixing, is a practical version of this, but it is not realistic to deduce quantitative values for the average length of the fine-grained intervals from the flatness-factor measurements. The zone averages of v flatness follow the total data quite closely,

whilst the u component falls off quite sharply. Both of these results are quite consistent with the description of the centre-line interaction already given.

The fact that the u and v flatness profiles of zone and total averages have only one peak (on the centre-line) agrees with the concept of a confined region of interaction, with a probability of finding both 'hot' and 'cold' fluid on the centre-line but not at the same time. The concept of 'time-sharing' in the core region of a pipe flow has been considered by Sabot & Comte-Bellot (1976), who have deduced an intermittent structure qualitatively similar to the present one, with "three states, two strongly stressed in opposite senses and one weakly stressed". Their work was based mainly on the behaviour of the instantaneous uv product, but although prediction of $\overline{uv}$ is one of the main aims of turbulence studies the instantaneous uv has some drawbacks as a test function for intermittency. First, uv is intermittent even in the fully turbulent part of a simple shear layer (Murlis 1975); second, uv near the centre-line of a pipe receives predominantly negative contributions from bursts moving in the $+y$ direction, predominantly positive contributions from bursts moving in the $-y$ direction, but predominantly *small* contributions from bursts moving in the z direction from the *sides* of the pipe. It is therefore not surprising that the uv bursts seen in the pipe are short, with long low-intensity regions separating them: the burst repetition wavelength of roughly one pipe diameter is of the same order as that deduced from observation of temperature traces in the present work. Sabot & Comte-Bellot's comments on the present model as briefly outlined by Bradshaw *et al.* (1973) result from too literal an interpretation of the phrase "alternations between positively- and negatively-stressed regions", which was an ellipsis for "predominantly-positive", etc., and not a statement that uv had a square-wave pattern.

6. Comparison with boundary-layer data

The physics of the interaction process have been discussed in some detail in the preceding sections. It now remains to relate these concepts to the turbulence structure as a whole and make a comparison with an ordinary boundary layer so as to test the superposition hypothesis. For this purpose the data of Klebanoff (1955) and Murlis (1975) have been used: both of these workers made turbulence measurements in a constant-pressure boundary layer, Klebanoff at a momentum-thickness Reynolds number of 7750 and Murlis at various Reynolds numbers up to 4750. At station E ($x/h = 26{\cdot}5$), just before the shear layers begin to merge, the momentum-thickness Reynolds number was 4450, permitting comparison with Klebanoff and Murlis. Murlis has used the first and second time derivatives of the instantaneous uv signal to determine the intermittency function, employing a digital analysis program developed from ours.

The most suitable shear-layer thickness for use in comparing a conventional boundary layer with, say, the 'hot' shear layer in a duct is one based on $\overline{\gamma uv_{\mathrm{H}}}$, which in the boundary layer would be identical with $\overline{uv}$. A thickness based on the intermittency or on some weighted integral of the shear-stress profile would avoid the effects of small local changes but for simplicity we have chosen δ_{05}, the distance from the surface at which $\overline{\gamma uv_{\mathrm{H}}}$ falls to 0·05 of its maximum value. In

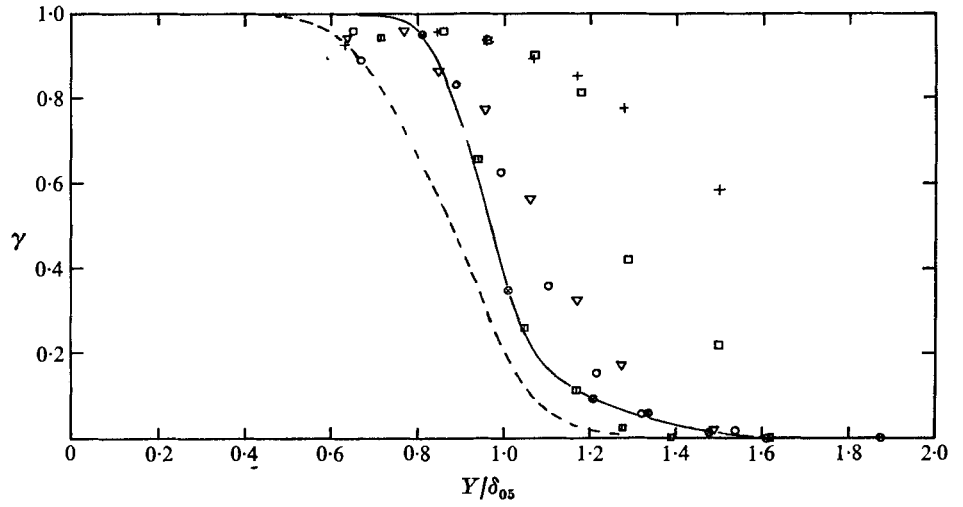

FIGURE 20. Intermittency profiles in the 'hot' layer compared with constant-pressure boundary layer (Klebanoff 1955). $Y = h - y$. ——, station E; - - - -, mean line through Klebanoff's data.

	⊗	⊞	⊙	▽	⊡	+
Station	*E*	*F*	*G*	*H*	*I*	*J*
x/h	26·5	32·6	38·7	44·8	50·9	57·0
δ_{995}/δ_{05}	1·020	0·965	0·977	0·959	0·957	0·890
δ_{05}/h	0·395	0·456	0·478	0·485	0·485	0·484

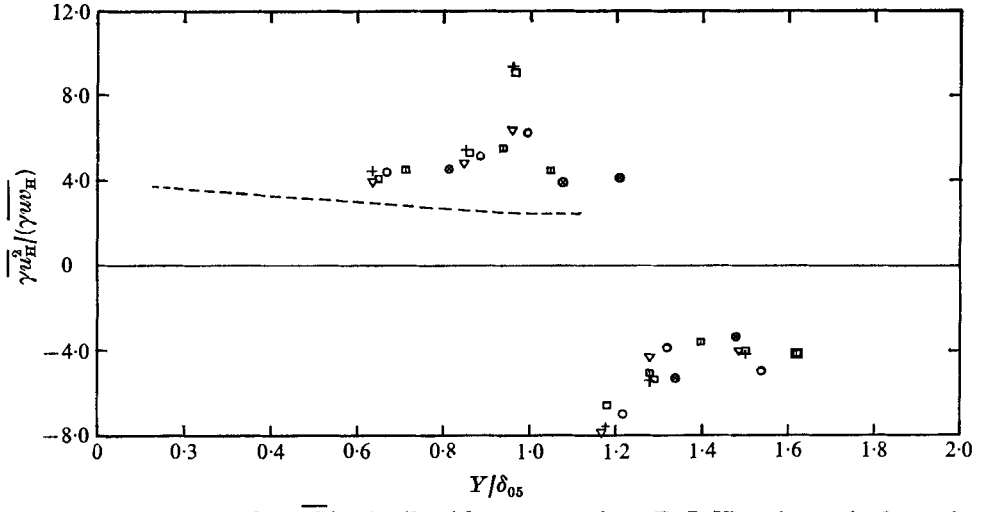

FIGURE 21. Dimensionless $\overline{u^2}$ in the 'hot' layer at stations E–J. Notation as in figure 20.

a boundary layer δ_{05} is close to δ_{995} (where $(U/U_e = 0{\cdot}995)$.

Values of δ_{05} have thus been obtained from the profiles of $\gamma\overline{uv}_H$, which, nearer the wall, should be equal to the total values. The very small extent of overlap in the zone-average profiles of $\overline{uv}$ leads to the rather surprising result that the representative thickness of the 'hot' layer is only 3% larger than the δ_{05} of

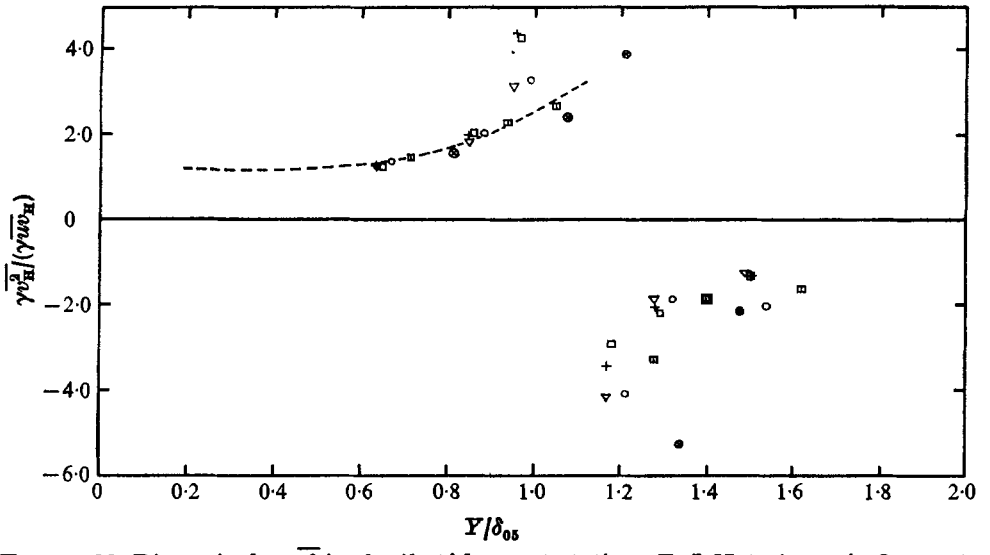

FIGURE 22. Dimensionless $\overline{v^2}$ in the 'hot' layer at stations *E–J*. Notation as in figure 20.

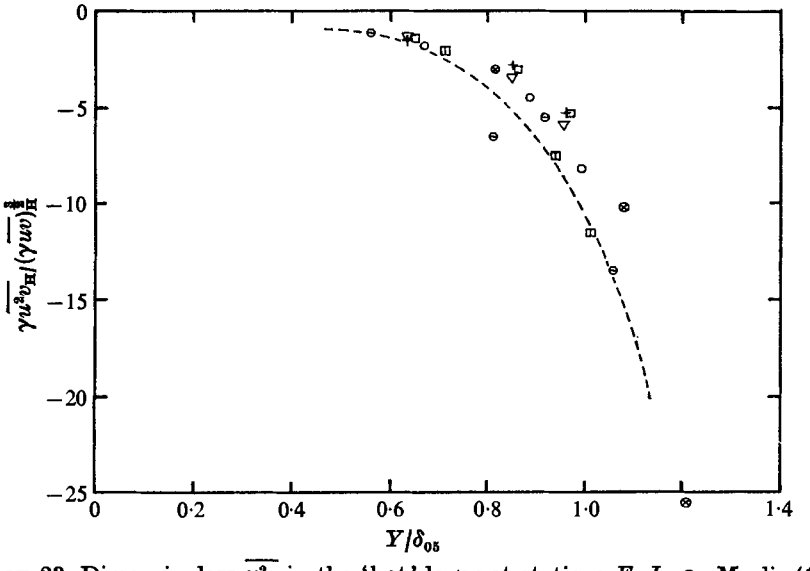

FIGURE 23. Dimensionless $\overline{u^2 v}$ in the 'hot' layer at stations *E–J*. ⊖, Murlis (1975); – – –, mean line through Murlis' data. Other notation as in figure 20.

the total shear-stress profile. Taking these values, the intermittency profiles have been plotted with respect to the 'hot' layer (i.e. with $Y = h - y$) in figure 20 non-dimensionalized by δ_{05}. Comparison with the constant-pressure boundary-layer data of Klebanoff (1955) shows that the slope of the duct flow profile at station *E* is rather steeper and the width of the intermittent region larger. In view of the discussion in §4, it is perhaps unreasonable to assess differences between two experiments using different techniques, but it is interesting to note

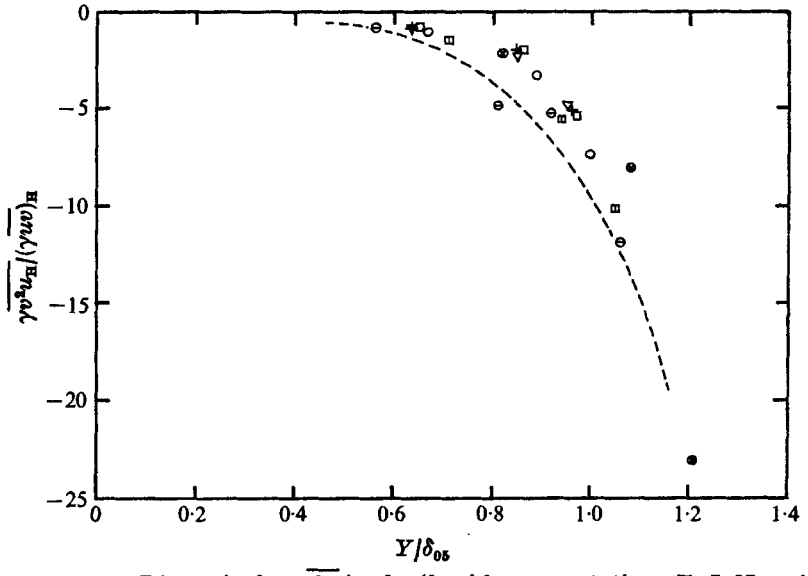

FIGURE 24. Dimensionless $\overline{v^2u}$ in the 'hot' layer at stations *E–J*. Notation as in figure 23.

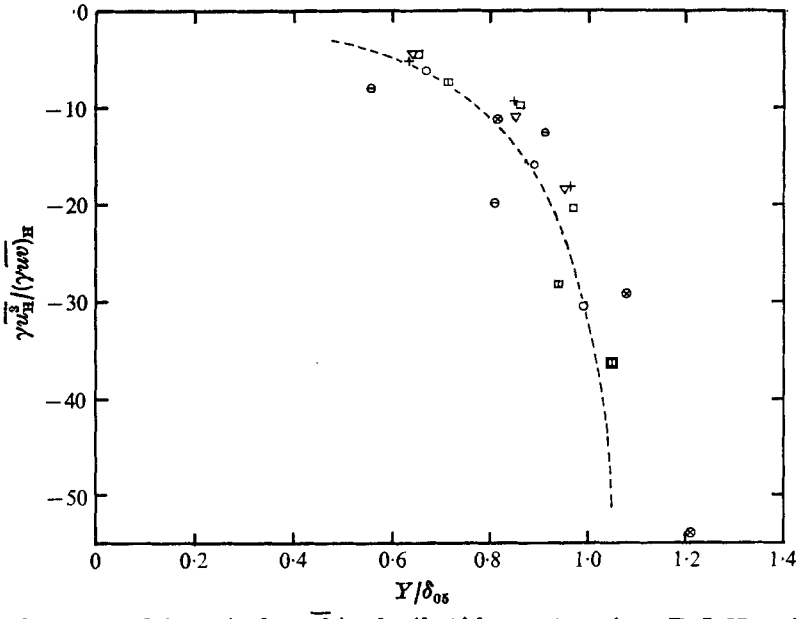

FIGURE 25. Dimensionless $\overline{u^3}$ in the 'hot' layer at stations *E–J*. Notation as in figure 23.

that Fiedler & Head (1966) found from their smoke photographs that the width of the intermittent region increased when the pressure gradient was favourable as it is in a duct.

In figures 21–26, the quantities $\gamma\overline{u_H^2}$, $\gamma\overline{v_H^2}$, $\gamma\overline{vu^2}_H$, $\gamma\overline{v^2u}_H$, $\gamma\overline{u_H^3}$ and $\gamma\overline{v_H^3}$ at different stations (all divided by appropriate multiples of $\gamma\overline{uv}_H$) are compared with

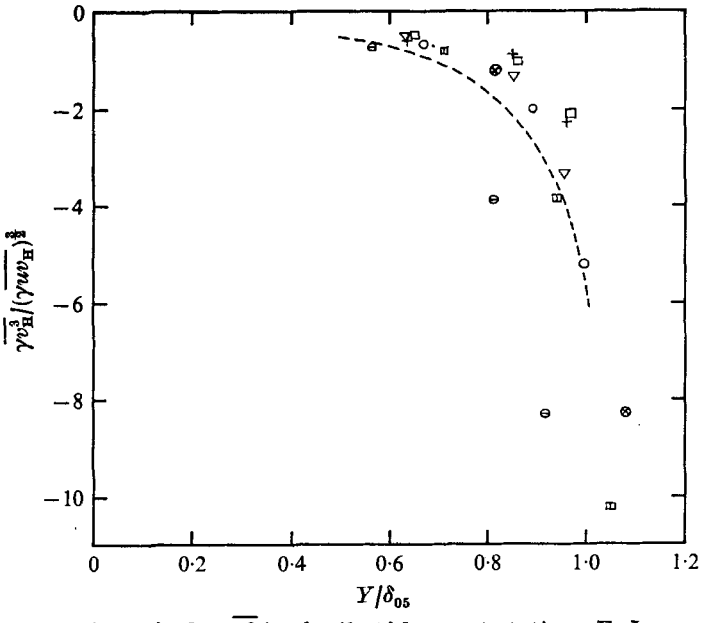

FIGURE 26. Dimensionless $\overline{v^3}$ in the 'hot' layer at stations *E–J*. – – –, mean line through Bradshaw's (1967) data. Other notation as in figure 23.

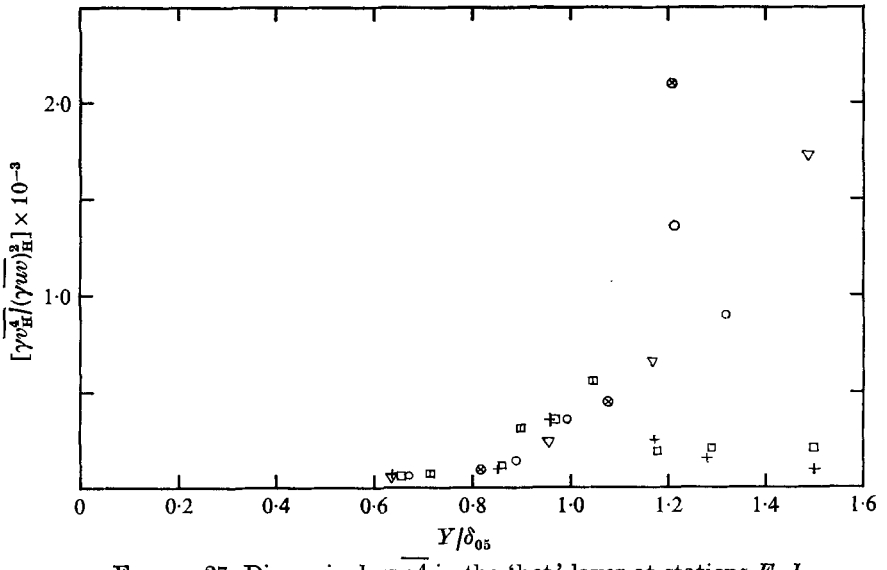

FIGURE 27. Dimensionless $\overline{u^4}$ in the 'hot' layer at stations *E–J*. Notation as in figure 20.

data from a constant-pressure boundary layer. Any significant effects of pressure gradient on the turbulence structure of the 'hot' layer, before the shear layers merge, would be expected to appear in the profiles of these dimensionless parameters at station *E*. However, the figures show fair agreement with the appro-

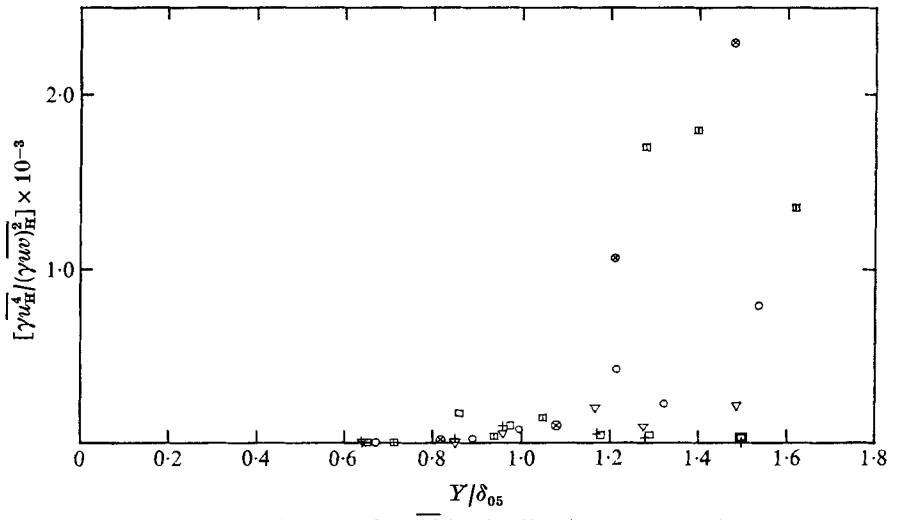

FIGURE 28. Dimensionless $\overline{v^4}$ in the 'hot' layer at stations *E–J*. Notation as in figure 20.

priate zone-average ('wholesale' intermittency) data of Murlis (1975) and also with the unconditional (ensemble) results of Klebanoff (1955) and Bradshaw (1967). The only noticeable difference seems to be that the triple products in the last-named paper are slightly higher than the duct results, particularly in the case of $\overline{v^3}$, which is perhaps consistent with a wider intermittent region.

7. The accuracy of superposition

The intermittency profiles at stations *E–J* are shown in figure 20 and indicate a reasonable collapse of data for stations *E–H*: stations *I* and *J* show the same trends as have already been observed in figure 4 and explained in previous sections. The apparent slight downstream increase in γ for each fixed Y/δ_{05} (where $Y = h - y$) is certainly due to similar measurement problems. However, the dimensionless quantities shown in figures 20–25 have all been calculated as the ratio of $\gamma \times$ 'hot' values and, if superposition is accurate, then profiles of these quantities should collapse at all downstream stations, even if γ is not quite correct.

Towards the outer edge of the boundary layer, $\overline{u^2}/\overline{uv}$ and $\overline{v^2}/\overline{uv}$ should increase: figures 21 and 22 demonstrate this effect with a satisfactory collapse of data in the 'hot' layer. The dimensionless triple products are essentially a measure of the diffusion of turbulent energy and shear stress across the layer. Figures 23–26 exhibit close agreement between measurements in boundary layer and duct for these quantities. The ratio obtained by dividing $\overline{u^4}$ by $(\overline{u^2})^2$ (or $\overline{v^4}$ by $(\overline{v^2})^2$), i.e. $\overline{u^4_H}/\gamma(\overline{u^2})^2_H$, will also show a satisfactory collapse of data and similarly for $\overline{u^3}$ (or $\overline{v^3}$) divided by $(\overline{u^2})^{\frac{3}{2}}$ (or $(\overline{v^2})^{\frac{3}{2}}$), i.e. $\overline{u^3_H}/\gamma^{\frac{1}{2}}(\overline{u^2})^{\frac{3}{2}}_H$. These are not however the u (or v) flatness and skewness factors of the 'hot' fluid when measured with

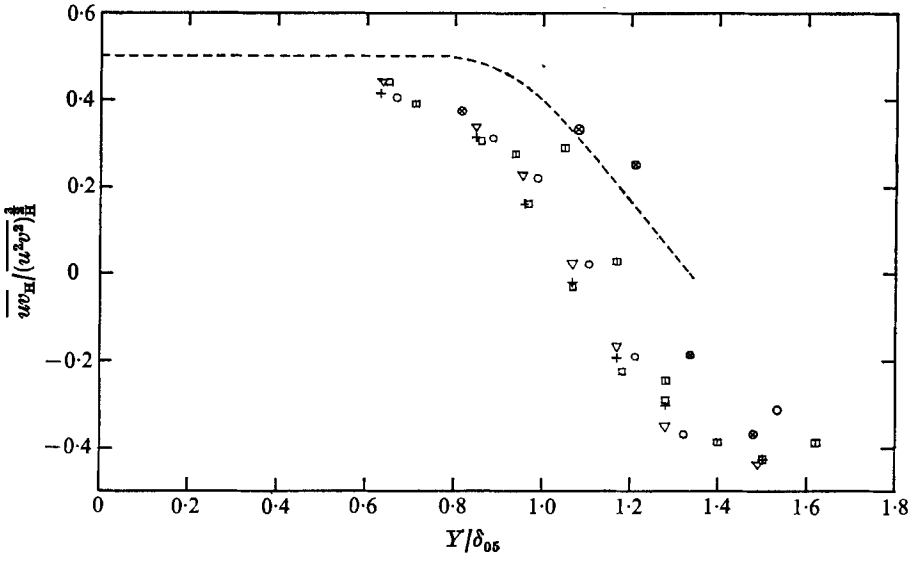

FIGURE 29. Shear correlation coefficient in the 'hot' layer at stations *E*–*J*. Notation as in figure 20.

respect to a common (total) baseline because the mean value of the fluctuating quantity u_H (or v_H) is non-zero [see (4): superposition implies $U_H \neq U$ anyway] but the correlation of profiles of these quantities at downstream stations in the interaction region shows support for superposition. It is of course possible to determine the discrete flatness and skewness of the 'hot' fluid alone using a regional baseline (figure 5) but this will supply no information with regard to superposition.

Finally, the shear-stress correlation coefficient (figure 29) is quite close to that for the constant-pressure boundary layer at station *E* but appears to fall off sooner when the layers begin to merge. This suggests that, during shear-stress reversal by fine-scale mixing, the entrained fluid reduces the local shear stress of the host layer (in this case the 'hot' layer), confirming the result observed in §5 that there is less overlap for $\overline{uv}$ than for $\overline{q^2}$.

8. Implications for calculation methods

The experimental results presented and discussed in the previous sections suggest that 'superposition' as a description of the interaction between the merging shear layers in a duct is a surprisingly good first approximation. One of the justifications for using this concept in the duct calculation method of Bradshaw *et al.* (1973) was that the turbulence intensity near the centre-line is quite low [$(\overline{u^2})^{\frac{1}{2}}/U \approx 0{\cdot}035$], so that the effects of any failure of the superposition hypothesis would be quite small anyway. The experimental data show that even percentage changes in turbulence structure are small but the results provide an opportunity to seek a second approximation, in which some of the more noticeable features of this weak interaction can be included in the calculation procedure.

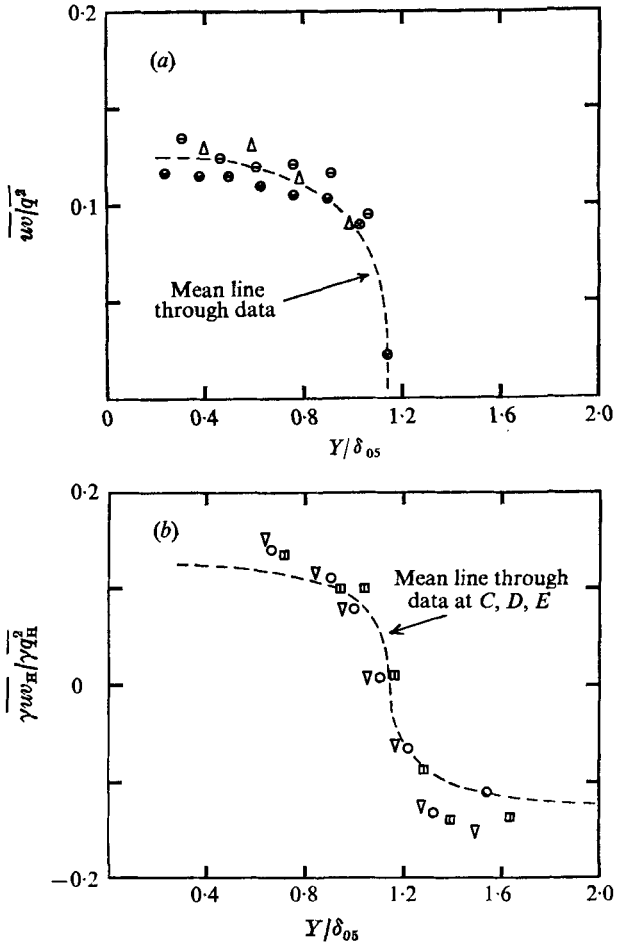

FIGURE 30. Values of $a_1 = \overline{uv}/\overline{q^2}$ (*a*) before the shear layers merge and (*b*) after the shear layers merge.

	△	⊖	⊗	◫	○	▽
Station	*C*	*D*	*E*	*F*	*G*	*H*
x/*h*	14·3	20·4	26·5	32·6	38·7	44·8

For example, the negative loop observed in the $\overline{uv}$ profiles (e.g. figure 8) is rather more significant than in any of the other antisymmetric quantities measured (see §5) and has been described as evidence of real interaction effects. The empirical assumption used by Bradshaw *et al.* (1967, 1973) is not very sensitive to changes in $a_1 = \overline{uv}/\overline{q^2}$, and $a_1 = 0{\cdot}15$ has been used with apparent success for both duct and boundary layer. The use of this parameter is therefore clearly justified by the experimental results presented in figure 30.

It should be noted that the different values of $a_1 = 0{\cdot}12$ before merging and 0·14 after (figures 30*a*, *b*) are unlikely to be caused by interaction but are most probably due to the different methods of measurement used for each set of data (results for stations *C*, *D* and *E* were obtained from analog devices and

while those for stations F, G and H were analysed digitally). Nor is there any additional significance in the satisfactory collapse of the data, for a_1 is merely the inverse sum of the $\overline{u^2}$ and $\overline{v^2}$ (and $\overline{w^2}$) dimensionless quantities, which are themselves shown to collapse well in figures 21 and 22. However, the negative loop in $\overline{uv}$ (figure 7) causes a_1 for the 'hot' layer to change sign near $Y = 1{\cdot}1\delta_{05}$ (figure 30*b*). Clearly 'hot' fluid is being occasionally found as far out as $1{\cdot}6\delta_{05}$ but the quantities are sufficiently small not to invalidate the choice of δ_{05} as a suitable length scale for the flow near the boundary-layer edge. Furthermore, the values of $\overline{uv}$ and $\overline{q^2}$ measured in these lumps of fluid are less than 0·5% of the maxima in each profile. It can therefore be concluded that the negative loops are unlikely to be significant in calculation methods.

It would be helpful in the development of a general prediction method to be able to define one or more interaction parameters applicable to a wide range of flows but probably having different values in each. These could be used in the calculation method to express some of the more obvious effects of interaction by correlating any changes in the empirical structure functions. Considering the shear-stress profiles discussed above, a possible choice might be the ratio $(\overline{uv})_{\mathrm{CL}}/(\overline{uv})_{\max}$, where CL denotes the centre-line for one layer. This is less than 0·1 in the duct but was found to be as high as 0·5 in the jet by Morel & Torda (1973), who applied the principle of superposition to plane jets, wakes and wall jets using the method of Bradshaw *et al.* (1967). Turbulent jet flows in general are bound to be a more severe test of superposition but Morel (1972) found that the changes in turbulence structure resulting from differences in the rate of growth of the different shear layers tend to obscure any failures of the superposition principle. For example, the ratio of the dissipation length parameter $L \equiv (\overline{uv})^{\frac{3}{2}}/$ dissipation to the local width of a turbulent jet in a moving stream depends quite strongly on the ratio of the centre-line velocity to the external stream velocity, which of course affects the growth rate $d\delta/dx$ even if the entrainment velocity is unchanged. Morel was able to correlate these and other differences with the growth rate, and showed that, with the possible exception of the energy diffusion, the turbulence structure functions used in his calculation method depended more on the growth rate than on whether the shear layer was a simple mixing layer or a jet or a wake. Some experimental work by Chaudhry (1973, unpublished work at Imperial College) on the interaction between two plane mixing layers at the end of the potential core of a two-dimensional jet shows very clearly how the departures from self-preservation spread outwards from the centre-line after the mixing layers meet, and the intensity near the centre-line is quite well predicted by the superposition principle, at least as far as 10 nozzle heights downstream.

9. Conclusions

Details have been presented of conditionally sampled measurements intended to explore the physics of the interaction process which takes place when the two internal boundary layers of a rectangular duct meet on the centre-line. It was

shown that the interaction is confined to within $\pm 0{\cdot}2h$ of the centre-line and consists of a continuously contorting interface, shaped by the eruption of eddies across the centre-line from either side of the duct (figure 6). The turbulent energy and shear stress of the intruding fluid, provided by diffusion from the regions of production nearer the wall, are attenuated by the action of fine-scale mixing. This centre-line interaction, once begun when the boundary layers merge, thus increases in strength until a steady rate of mutual eddy intrusion and fine-scale mixing is achieved, when the flow is commonly called 'fully developed'.

By plotting profiles of intermittency-weighted dimensionless parameters, the turbulence of one of the layers was compared with data measured in a constant-pressure boundary layer. The analysis showed that the influence of the favourable pressure gradient on the turbulence structure of the duct shear layers before merging was not very significant, and during interaction the profiles of the dimensionless parameters at different streamwise distances were found to collapse without much scatter around the constant-pressure boundary-layer data. This appeared to support the hypothesis that the turbulence fields of the two shear layers may be simply superposed, interacting only through the mean velocity profile. Departures from superposition seem to be essentially determined by the process of fine-scale mixing which takes place at the boundaries of large eddies which continually erupt a small distance across the centre-line from either side of the duct. It was concluded that superposition is a good first approximation in duct flow where the level of turbulence is low and it is most unlikely that other types of interaction will be so much stronger as to invalidate superposition as a first approximation: at most, it is possible that the empirical functions will depend weakly on interaction parameters like $\overline{uv}_{\mathrm{CL}}/\overline{uv}_{\max}$ in one layer and a relatively small amount of additional data should suffice to establish this dependence to the accuracy required.

This work was supported by the Science Research Council, grant no. B/SR/8978. We are grateful to Dr C. W. Van Atta for advice on digital data processing and to Dr A. Brandt for extensive help with programming.

REFERENCES

ANTONIA, R. A. 1974 *Proc. 5th Int. Heat Transfer Conf., Tokyo*, vol. 2, p. 95.

ANTONIA, R. A., PRABHU, A. & STEPHENSON, S. E. 1975 *J. Fluid Mech.* **72**, 455.

BRADSHAW, P. 1967 *J. Fluid Mech.* **30**, 241.

BRADSHAW, P. 1971 *An Introduction to Turbulence and its Measurement.* Pergamon.

BRADSHAW, P., DEAN, R. B. & MCELIGOT, D. M. 1973 *J. Fluids Engng, Trans. A.S.M.E.* **95**, 214.

BRADSHAW, P., FERRISS, D. H. & ATWELL, N. P. 1967 *J. Fluid Mech.* **28**, 593.

BRADSHAW, P. & MURLIS, J. 1974 *Imperial College Aero. Rep.* no. 74–04.

BRANDT, A. & BRADSHAW, P. 1972 *Imperial College Aero. Rep.* no. 72–11.

BREMHORST, K. & BULLOCK, K. J. 1970 *Int. J. Heat Mass Transfer*, **13**, 1313.

BOURKE, P. J. & PULLING, D. J. 1970 *Int. J. Heat Mass Transfer*, **13**, 1331.

CHANDRSUDA, C. 1976 Ph.D. thesis, Imperial College, London University.

CHARNAY, G., COMTE-BELLOT, G. & MATHIEU, J. 1972 *C. R. Acad. Sci. Paris*, A **275**, 615.

CORRSIN, S. 1949 *N.A.C.A. Tech. Note*, no. 1864.

DEAN, R. B. 1974*a* Ph.D. thesis, Imperial College, London University (available on microfiche from Aero. Dept. Imperial College).

DEAN, R. B. 1974*b* *Imperial College Aero. Rep.* no. 74-12.

FIEDLER, H. & HEAD, M. R. 1966 *J. Fluid Mech.* **25**, 719.

GIBSON, C. H. 1973 *Agardograph*, no. 174.

GUITTON, D. E. & PATEL, R. P. 1969 *McGill Univ. MERL Rep.* no. 69–7.

HEDLEY, T. B. & KEFFER, J. F. 1974 *J. Fluid Mech.* **64**, 645.

JOHNSON, D. S. 1959 *J. Appl. Mech. Trans. A.S.M.E.* **81**, 325.

KLEBANOFF, P. S. 1955 *N.A.C.A. Rep.* no. 1247.

LARUE, J. C. 1973 Ph.D. thesis, University of California.

LARUE, J. C. & LIBBY, P. A. 1974 *Phys. Fluids*, **17**, 873.

MOREL, T. 1972 Ph.D. thesis, Illinois Institute of Technology.

MOREL, T. & TORDA, T. P. 1973 *A.I.A.A. J.* **12**, 533.

MURLIS, J. 1975 Ph.D. thesis, Imperial College, London University.

PHILLIPS, O. M. 1955 *Proc. Camb. Phil. Soc.* **51**, 220.

REICHERT, J. K. & AZAD, R. S. 1976 *Can. J. Phys.* **54**, 268.

SABOT, J. & COMTE-BELLOT, G. 1976 *J. Fluid Mech.* **74**, 767.

THOMAS, R. M. 1973 *J. Fluid Mech.* **57**, 549.

WEIR, A. D. & BRADSHAW, P. 1974 *Imperial College Aero. Rep.* no. 74-09 (replaces no. 72-11).

WYNGAARD, J. C. 1971 *Phys. Fluids*, **14**, 2052.